X-693-74-316

PREPRINT

NASA TM X- 70789

INTERSTELLAR SCATTERING OF PULSAR RADIATION

I. SCINTILLATION

D. C. BACKER

NOVEMBER 1974

GSFC — GODDARD SPACE FLIGHT CENTER

GREENBELT, MARYLAND

"This paper presents the views of the author(s), and does not necessarily reflect the views of the Goddard Space Flight Center, or NASA."

For information concerning availability of this document contact:

Technical Information Division, Code 250
Goddard Space Flight Center
Greenbelt, Maryland 20771

(Telephone 301-982-4488)

INTERSTELLAR SCATTERING OF PULSAR RADIATION

I. SCINTILLATION

D.C. Backer*
Goddard Space Flight Center
Greenbelt, Maryland

Running Title: Interstellar Scattering of Pulsars.

Address Proofs to: Code 693, Goddard Space Flight Center
Greenbelt, Maryland 20770
U.S.A.

Subdivision: 2. Galactic Structure, Stellar Dynamics, Interstellar Matter.

Main Journal

D. C. Backer, Code 693
Goddard Space Flight Center
Greenbelt, Maryland 20770
U.S.A.

*NAS/NRC Resident Research Associate

ABSTRACT

An investigation of the intensity fluctuations of 28 pulsars near 0.4 GHz indicates that scintillation spectra have a Gaussian shape, scintillation indices are near unity and the scintillation bandwidth depends linearly on dispersion measure. Observations near 2.5 GHz suggest a strong dependence of the frequency at which scintillation indices fall below unity on dispersion measure. Recent multistation measurements of scintillation provide values or limits for the scale size of the scattering diffraction pattern. The dependences of scattering parameters on dispersion measure is discussed in terms of the current models. It is suggested that any line of sight through the galaxy encounters increasingly-rare, increasingly-large deviations of thermal electron density on the scale of 10^{11} cm.

Key Words: Scintillation, interstellar medium, pulsars.

I. INTRODUCTION

Scheuer (1968) and Salpeter (1969) interpreted the rapid, narrow-bandwidth, random fluctuations of pulsar signals first observed by Hewish and his colleagues (1968) as the result of scattering by minute density irregularities in the column of interstellar thermal electrons that was known at the time to disperse the pulsed signals. Rickett (1970) extended the model of Scheuer using the work by Ucsinski (1969) and made a detailed comparison of his observations to the theory. Mutel et al. (1974) have recently discussed power-law density irregularity spectra in the interstellar medium based on the work of Salpeter and Lovelace (1970). Cohen and Cronyn (1974) describe observable consequences of interstellar scattering based on current data and theory. In the models the thermal plasma is assumed to be uniformly distributed on a galactic scale, with rare exceptions, since HI absorption measurements for pulsars provide distance estimates which, with the electron column densities (dispersion measures DM), yield comparable average electron densities along different lines of sight (Gordon and Gordon 1973, Gomez-Gonzalez and Guelin 1974). Also, pulsars lie below a line $DM \propto \csc(|b|)$ in the -DM galactic latitude(b) plane (Hewish 1970, Condon and Backer 1974), and above a line $L \propto DM^2$ in the Luminosity(L)-DM plane (Comella 1973); both of these results lend support to the idea that the dispersing plasma is distributed generally in the interstellar medium. The distribution of irregularities within

the dispersing plasma is also probably general in the sense of frequent, on the scale of 10 pc, perturbations of the electron density as discussed by Salpeter, rather than in the sense of isotropic turbulence. Scheuer and Salpeter considered thin-screen approximations to interstellar scattering, while Rickett applied the work of Uciński which deals with extended screen effects.

The rare exceptions mentioned above are the thermal plasmas in the Crab nebula, in the Gum nebula, and in miscellaneous HII regions (Prentice and ter Haar 1969). Although Gomez-Gonzalez and Guelin (1974) do not find a dependence of the mean electron density on distance, the average perturbation of the density about the mean could increase with distance as the line of sight intersects increasingly-rare, increasingly-large deviations of the electron density, particularly in directions toward the galactic center.

The frequency dependence of scattering parameters (Rickett 1970, Lang 1971, Rankin et al. 1970, Komesaroff et al. 1970, Backer 1974, Mutel et al. 1974) is consistent both with Scheuer's model which assumes a homogeneous and isotropic medium and a Gaussian irregularity spectrum and with Salpeter's model which includes the effects of a density irregularity spectrum with a logarithmic slope of $S = 4$ (see Mutel et al.). The frequency dependence of the extended-screen model (Rickett 1970) is also in agreement with the observations. The dependence of the scattering parameters on distance, or dispersion measure for a uniform interstellar medium, is less clear. Only one parameter, the correlation bandwidth (B_s),

or its Fourier transform conjugate the pulse broadening time, is clearly dependent on dispersion measure (Rickett 1970, Sutton 1971). Rickett finds a relation of $B_s \propto DM^{-2}$ which is consistent with the above models, while Sutton (1971) finds a trend of $B_s \propto DM^{-4}$. In this paper we investigate the dependence of other scattering parameters on dispersion measure: the correlation time (scintillation bandwidth), the diffraction pattern spatial scale, and the critical frequency for scintillation. Before presenting these we discuss the shape of scintillation spectra. Additional topics are given: the use of scintillation of mainpulse and interpulse radiation as a means of resolving the transverse separation of the two emitting regions, and a simulation of scintillation using a computer code developed by R. Lovelace (1974). Finally we discuss the observed strong dependence of scattering parameters on dispersion measure and present a model scintillation spectrum with explicit dependence on DM and radio frequency.

II. OBSERVATIONS

Pulsar recordings extending over intervals ranging from an hour to several days were made over the past few years at several observatories (National Radio Astronomy Observatory[1], Jodrell Bank and Arecibo Observatory) to investigate pulse-to-pulse fluctuations, flux-density spectra, interstellar scattering diffraction patterns, individual pulse polarization phenomena and differential positions. Table 1 summarizes these experiments. This paper presents the salient

[1]NRAO is operated by Associated Universities, Inc., under contract with the U.S. National Science Foundation.

features of interstellar scintillation contained in this large collection of data. Other papers have discussed or will discuss the individual experiments with more detail, although relevant aspects of some observations not given in table 1 will be presented in the succeeding sections of this paper. All the data described in table 1 provided the author with experience on the fluctuations of pulsar signals; only part of the data will be discussed here due either to the redundancy of the information, to the incompatability of magnetic tape formats, or to the fact that the radiometer bandwidths or the lengths of recording were insufficient for the analysis of scintillation.

III. SHAPE OF SCINTILLATION SPECTRUM

The shape of the scintillation spectrum, which gives the variance density of scintillation as a function of fluctuation frequency for a pulsar, is confused at some level by the variability of the emitted radiation, due to changes of parameters intrinsic either to the pulse emission mechanism or to propagation conditions in the near pulsar environment. Variance-density spectra of pulsar data typically have the following constituents (Lovelace and Craft 1968, Backer 1973) which are labeled in a schematic spectrum in figure 1:

(a) a rapid decrease near zero, followed by

(b) a slower decrease out to a point which varies from 0.1 to 0.5 cycles per pulse period (c/P_1), and beyond which

(c) a constant, or "white", level is found with

(d) one or more quasiperiodic features superposed on the above "continuum",

Additional increases in pulsar spectra below frequencies of inverse weeks (2×10^{-6} Hz), which have been observed at meter wavelengths (Cole, Hesse and Page 1970, Huguenin *et al.* 1973), will not be discussed here. Constituents (c) and (d) are properties of the pulsar since their corresponding temporal fluctuations are correlated over broad bandwidths, are related to complex changes in total-intensity and polarization emission waveforms unlike the random variations expected from scintillation, and are in case (d) periodic. Rickett (1970) and Lang (1971) showed that constituent (a) is dependent on dispersion measure(DM), and therefore to be identified with scintillation arising in the interstellar medium: they found that the fluctuations producing (a) are reduced considerably by observations with a radiometer bandwidth exceeding a characteristic correlation bandwidth B_s which varies with DM^{2-4} (see also Sutton, 1971).

Since finite lengths of data are used to estimate pulsar fluctuation spectra, the sampling function could lead to a spurious component (b) due to the excess modulation at low frequencies. This is judged not to be a serious problem based both on observations of constituent (b) when scintillation has been removed by the use of large radiometer bandwidths and on computer simulations of scintillation records which are discussed in VIII. Often constituent (b) can be identified with intrinsic variability when the fluctuations are related to deep and

abrupt nulls (Backer 1970a), equally abrupt mode changes (Backer, 1970b, Lyne 1971), isolated bursts of emission (Huguenin, Taylor and Troland 1970, Backer, Rankin and Campbell 1974), and low-frequency periodicities (Lang 1969), most of which are correlated over hundreds of MHz. This constituent usually follows an exponential decrease from zero frequency, and is often sufficiently strong to confuse measurements of scintillation time scales. Thus a careful inspection of the low-frequency end of a spectrum is needed to determine the shape of the scintillation spectrum. One can be guided by the hypotheses that (i) scintillation spectra will be Gaussian for interstellar electron-density spectra which are consistent with a radio-frequency (ν) dependence of the correlation bandwidth B_s, or the inverse of the pulse-broadening time, of ν^4 (Rickett 1970, Rankin et al. 1970, Komesaroff et al. 1970, Lang 1971, Backer 1974), and of the scattering angle of ν^{-2} (Mutel et al. 1974, Vandenberg 1974); (ii) normalized spectra should have unit area corresponding to strong scattering in the Fraunhofer, or far field, limit; and (iii) any consistent measure of the width of the spectra should decrease with ν and increase with DM^{α}, where α is 0.5 for constant motion of the observer relative to a uniform medium of Gaussian irregularities (Scheuer 1968) or for the power-law irregularity spectra discussed by Salpeter (1969) with S = 4 as required by the above dependences on radio frequency.

A study of the spectra of 28 pulsars at radio frequencies near 400 MHz, which is presented in §IV, reveals that constituent (a)

exists in all but three cases for which either the length of the recordings was too short or the radiometer bandwidth was too large to observe scintillations. Furthermore, in many cases the exponential constituents are weak enough to fit Gaussians to the scintillation spectra over several octaves of fluctuation frequency, from a few percent of the e^{-1} width, f_e, out to $\sim 2\ f_e$.

In figures 2 to 4 variance-density spectra are given for three pulsars. In these plots both high and low resolution spectra are given with Gaussian curves (dash-dotted), selected by eye from a template of curves, drawn through the low frequency ends of the high-resolution spectra (solid). The low-resolution spectra (dashed) provide comparison levels, the levels of uniform, or "white", fluctuations at, or near, the Nyquist limit. Error bars indicate the uncertainties expected due to limited smoothing of adjacent points in the spectra. For PSR 0823+26 (fig. 2) the high-resolution spectrum from 408-MHz data decreases to the instrumental noise level, rather than to the level of the white fluctuations given by the companion low-resolution spectrum based on 430-MHz data. In the other two cases instrumental noise is insignificant. These variance-density spectra are defined in an absolute manner to allow comparison at other radio frequencies or other epochs. Comparison functions are given in figure 5 from 2695-MHz data recorded in 1973 May (see table 1). For PSR 0329+54 the width of the scintillation portion of the spectrum is scaled down from the 408-MHz result in proportion to the ratio of the radio frequencies as expected; the area of the scintillation spectrum

corresponds to a scintillation index of only 0.4 which is small compared to the expected value of unity. Scintillation at 2695 MHz is discussed in more detail in §V, and scintillation index variability is discussed in §VIII. The level beyond the scintillation portion, $f > 0.3$ mHz, is higher than that expected based on the 408-MHz data above 3 mHz (fig. 2) which suggests either an exponential constituent of fluctuations or a radio-frequency dependence of the continuum level. The 2695-MHz variance-density spectrum for PSR 0823+26 has a scintillation portion which agrees with the 408-MHz data (fig. 3) based on the conventional notions of frequency scaling described above. The level beyond the scintillation portion is undetermined due to instrumental noise and the low Nyquist frequency. The 2695-MHz spectrum for PSR 1133+16 has a scintillation portion which also agrees with the 408-MHz data, if account is taken of both weak scattering (see §V) and the level and slope of the portion of the exponential constituent of the 408-MHz spectrum just beyond 3.5 mHz (fig. 3).

Further support to the argument that the exponential constituents of pulsar variance-density spectra are due to "intrinsic" causes is that neither the transition point where the Gaussian scintillation spectra and the exponential constituent are equal, nor the absolute level of the exponential constituent bear any relationship to dispersion measure for the sample of 28 objects discussed here. In contrast, the width of the Gaussian portion does depend on dispersion measure as shown in the following section.

It is concluded that all pulsar data are consistent with a Gaussian shape and unit area for the normalized, variance-density spectra of interstellar scintillation. There is no evidence for the nongaussian behavior discussed by Little and Matheson (1973) based on the work of Lang (1971).

IV. WIDTH OF SCINTILLATION SPECTRA

Rickett (1970) measured scintillation time scales, t_x, for 12 pulsars from the separation of peaks on analog recordings and found, roughly, an inverse relation between t_x and DM. There are several reasons not to expect a rigid relationship:

(a) insufficient data for a stationary result;

(b) nonuniform medium of irregularities in electron density; and

(c) variation from object to object of the transverse velocity (or velocities?) of the scattering medium with respect to the line of sight to the pulsar.

The recordings near 400 MHz listed in table 1 were analyzed to identify the scintillation spectra, as discussed in the preceeding section, and then to measure the areas, μ^2, and the widths at e^{-1}, f_e, of the Gaussian scintillation spectra. The results are summarized in table 2 which gives systematic pulsar names (PSR), periods (P), dispersion measures (DM), lengths of recording in periods (N x M, where N is the number of samples and M is the sampling interval), square roots of the areas of the scintillation spectra (μ, the scintillation index), e^{-1} widths of the scintillation spectra (f_e), transition

frequencies where the scintillation spectrum and the intrinsic spectrum are equal (f_t), sources of the data by observatory (AO = Arecibo Observatory, GB = Green Bank, JB = Jodrell Bank) and by experiment (FF = fluctuation, IS = scattering, PN = polarization), and the qualities of the measurements ($f_e \times N \times M \times P = f_e \times T$). Copies of the spectra may be obtained from the author upon request.

The values of f_e from table 2 are plotted against dispersion measure in figure 6. Only upper limits were obtained for PSR's 1541+09, 1604-00 and 1944+17 due either to the brevity of the recordings or to the narrowness of the correlation bandwidth relative to the radiometer bandwidth. A value of f_e for PSR 0833-45 (DM $\sim$ 70 pc cm^{-3}) at 408-MHz is included in figure 6 based on work at 834 MHz (Backer 1974).

The trend of the 400-MHz data is given by

$$f_e = 0.04 \text{ DM } \nu^{-1} \text{ MHz}, \quad (1)$$

where DM is given in units of pc cm^{-3} and ν in GHz here and in following equations; individual points are spread by a factor of three from this trend due either to large scale ($\sim$ 100 pc) inhomogeneities of the scattering material or to discordant velocities as discussed at the beginning of this section. This strong dependence of f_e on DM evident in figure 6 is not expected within the context of uniform-medium models of scattering. Further discussion may be found in §IX.

V. THE CRITICAL FREQUENCY FOR SCINTILLATIONS

Observations of scintillation at meter wavelengths are consistent with scintillation indices of unity (see §IV and references therein). Indices of one are expected when (i) random-phase deviations imposed on a plane wave by the interstellar electron-density irregularities are many radians, and (ii) the observer is sufficiently far from the density, or phase, irregularities to allow the reception of scattered radiation from many paths. At some radio frequency for any object, the critical frequency, one of these conditions will be violated, and the scintillation index will drop below unity. For a collection of objects, at a given radio frequency, the index will fall below unity for objects closer than some critical distance, or dispersion measure, assuming a uniform medium. Explicit statements of the above conditions involve the product $DM^{\alpha} \nu^{\beta}$ with $\alpha_1 = 1/2$ and $\beta_1 = -1$ for condition (i) and $\alpha_2 = 1/2$ and $\beta_2 = -2$ for condition (ii). Thus, given the critical dispersion measure for weak scintillation DM_c at some radio frequency ν, one can obtain the critical frequency ν_c as a function of DM for the above models.

Downs and Reichley (1971) were first to show that at least one of the conditions above was violated for some objects at 2385 MHz. Their scintillation indices are upper limits for interstellar scintillation, since they did not consider contributions from intrinsic effects (§III). Their data are given as published in figure 7(●). Indices have also been estimated from the scintillation portions of

variance-density spectra of the 2695-MHz data listed in table 1. The results are listed in table 3 and plotted in figure 7 for the 1973 May flux-density experiment (A and ✱) and the 1974 May position experiment (B and ▲). The latter data sets extended over longer periods of time than the former and therefore are probably more reliable when available. For PSR's 0833-45, 1749-28, and 1933+16 the correlation bandwidths are known (Sutton 1971, Backer 1974) and corrections to the indices for bandwidth suppression have been applied (□).

Below the critical dispersion measure, at a given radio frequency such as 2695 MHz, the scintillation index will decrease in proportion to DM^{α} where α is 1/2 if condition (i) is violated and 1 if both conditions are violated, or if condition (ii) is violated sufficiently strongly (Lovelace 1970). A simple model of this cutoff is

$$m = \frac{1}{1 + (DM_c/DM)^{\alpha}} \qquad (2)$$

The data is not sufficient to determine α within the range of 0.5 to 1.0 discussed above, although it appears that a value closer to 1 than to 0.5 is favored with $DM_c \tilde{=} 5$ pc cm^{-3} (see fig. 7). Taking $\alpha = 1$ and $\beta = 1$ (arbitrarily), one finds that the critical radio frequency for scintillations will vary as

$$\nu_c = 0.5\ DM\ GHz, \qquad (3)$$

although both the constant and the dependence on DM are clearly uncertain from the above discussion.

In 1974 May 53 objects were observed at 775, 968 and 1440 MHz over an eight-day interval (table 1). At each frequency three or four measurements of pulse energy, averaged over about four minutes, were obtained on as many separate days. For objects with dispersion measures less than ~25 pc cm^{-3} the correlation bandwidths of scintillation exceed the radiometer bandwidth of 20 MHz and therefore the samples are independent realizations of scintillation plus day-to-day intrinsic variations. For objects with dispersion measures exceeding ~80 pc cm^{-3}, the scintillations are quenched by the radiometer bandwidth and the samples exhibit only the day-to-day variations. (The data for objects with DM ~80 pc cm^{-3} confirm the steep dependence of correlation bandwidth on DM discussed by Sutton (1971)). Since in the latter case (DM > 80 pc cm^{-3}) the rms deviations about the mean pulse energy are less than 0.2 times the mean, we conclude that the rms deviations of the former group, DM < 25 pc cm^{-3}, are dominated by interstellar scintillation. Figure 8 gives the radio frequency dependences of the rms deviations for nine objects with DM < 13 pc from the 775-1440 MHz experiment and from the data in tables 2 and 3 at 400 MHz and 2695 MHz, respectively. This figure confirms the existence of a critical frequency for scintillations and suggests that the constant in equation (3) should be closer to 0.1. Equation (3) is probably accurate enough to indicate that it will be difficult to study many pulsars in the weak scintillation regime.

VI. SCATTERING DIFFRACTION PATTERN SCALE

The intensity diffraction pattern produced in the plane of the observer by interstellar scattering below the critical frequency of a point source of unit strength may be described by its wave number spectrum

$$M(\underset{\sim}{q}) = \exp[-a^2(q_x^2 + q_y^2)/2], \tag{4}$$

where a is the scale size of the diffraction pattern and $\underset{\sim}{q} = (q_x, q_y)$ is the vector wave number. The gaussian shape of $M(\underset{\sim}{q})$ is inferred from the gaussian shapes of the variance-density spectra $D(f)$ described in §III under the simple assumption that a scintillation time and a pattern wave number are related by a speed. With this assumption, the following relations hold:

$$\begin{array}{ccc} D(f) & \longleftrightarrow & D(\ ) \\ \updownarrow & & \updownarrow \\ M(\underset{\sim}{q}) & \longleftrightarrow & M(\underset{\sim}{r}), \end{array} \tag{5}$$

where $\longleftrightarrow$ refers to Fourier tranformation and $\Leftrightarrow$ refers to a one-dimensional integration along the coordinate perpendicular to the pattern velocity $\underset{\sim}{u}$ and to a change of variables $2\pi f/|\underset{\sim}{u}| = q$. The size a varies as $DM^{-1/2}\nu$ for the uniform-medium models of Scheuer (1968) and Salpeter (1969). Multiple station measurements of pulsar scintillation are consistent with values of $M(\underset{\sim}{r})$ which are less than unity: Slee *et al.* (1974) observed seven objects at 327 MHz with $|\underset{\sim}{r}| = 8000$ km, and the unpublished results of Backer, Lyne and Zeissig at 408 MHz with $|\underset{\sim}{r}| \leq 5500$ km (table 1) are consistent with those of Slee *et al.* We estimate a from these observations to be

(6) $$a = (1.4\ ^{+2.5}_{-0.5}) \times 10^{10}\ DM^{-1/2}\ cm,$$

although, given the results of §§IV and V, a stronger dependence on DM might be expected. Equation (6) is valid for $\nu < \nu_c$; when $\nu > \nu_c$ one may substitute $\nu = \nu_c$ into equation (6). The uncertainty in $\underline{a}$ is based on the paucity of measurements and, presumably, on inhomogeneities of the scattering.

VII. SCINTILLATION OF MAINPULSE AND INTERPULSE EMISSION

Investigations of ionospheric and interplanetary scintillations have often been a battle to separate medium effects from source structure effects since the "resolving power" of these scintillations is in the same regime as the angular structure of many extraterrestrial, natural sources. The situation is further confused by the time-variable properties of these scattering media. The "resolving power" of the interstellar medium is generally thought to fall in the range where incoherent radio sources at the present level of detection are relatively large, and therefore do not scintillate, and all pulsar emitting regions (and perhaps some molecular-line masers) are relatively small, and therefore scintillate 100 per cent below the critical frequency (§V). We explore the first point elsewhere (Lovelace and Backer 1972, Condon and Backer 1974) and the second point below.

The resolving power of the interstellar medium compared to an angular size scale for a pulsar emission region may be expressed as the ratio of twice the scattering diffraction pattern scale (§VI) to the light cylinder radius of the pulsar, $r_c = c\ P/2\pi$,

(7) $$2\ a/r_c = 6\ DM^{-1/2}\ \nu\ P^{-1}.$$

This ratio is 0.6 for ν = 0.4 GHz, DM = 16 pc cm^{-3}, and P = 1 sec. Thus sources of pulsar radiation from any one pulsar which are distributed over a distance r_c at the time of emission to the observer can be distinguished by their independent scintillations. One is essentially collecting radiation scattered by many irregularities in the intervening medium with propagation paths which are phase stable for one period so that differential positions can be obtained for radiation arriving at different times in the pulse period in a manner analagous to long-baseline interferometry. Most pulsar radiation is confined to a few per cent of the period and therefore is probably from a source distributed over not more than a few per cent of pulsar latitude and longitude. However, several of the short-period objects have interpulse emission which is spaced roughly 180 degrees of longitude, as observed, from the mainpulse emission region (Backer, Boriakoff and Manchester 1973 and references therein). The two regions then could be displaced in latitude by an angle such as twice the angle between the magnetic dipole axis and the rotational axis, θ. The regions, when emitting to the observer, would be displaced by 2 r tan θ, where r is the distance from the center of mass of the pulsar to the emitting region, $r \leq r_c$.

For PSR 0823+26 and PSR 1929+10 there was no evidence for independent scintillations of the mainpulse and interpulse emissions in the relatively short recordings of the Arecibo polarization survey at 430 MHz (table 1). This observation sets limits of 1.2 and 8.0 r_c, respectively, on the separation of the emitting regions at the time of

emission. These limits are not interesting for discussions of pulsar emission. Indeed, one can only improve them (i) by observing at lower radio frequencies where sensitivity would be a serious problem, or (ii) by observing higher dispersion measure objects, such as PSR 1055-51 (McCulloch et al. 1974) which has a strong interpulse, but a short period (eq. (7)), or (iii) by finding longer-period objects with interpulses such as the elusive (or dead?) PSR 0904+77 which may have an interpulse and a period of 1.5 s, but which has not been detected since the months of its discovery (Taylor and Huguenin 1969).

The problem can be turned around in the case of a short-period binary pulsar (Taylor and Hulse 1974). In this case we know the path of the radiation source and can probe in principal the stability of the dispersing and scattering medium during an orbit.

VIII. COMPUTER SIMULATION OF SCINTILLATION

R. Lovelace (1974) has developed a computer code to simulate far-field scattering from a one-dimensional thin screen with an arbitrary spectrum of phase fluctuations. A version of this code has been developed to look at the intensity fluctuations from a scattering screen with a gaussian distribution of phase fluctuations whose root-mean-square (rms) deviation from zero is 20 radians and whose scale size is 10^{11} cm at a distance of 500 pc and at a radio frequency of 0.4 GHz. The intensity data in the observer's plane resulting from illuminating this screen with a plane wave was broken into sections, in an attempt to mimic actual observations with $f_e\ T \sim 5$ as discussed in §§III and IV. In each section a scintillation index and bandwidth was determined. We found that the scintillation index is less well-defined than the scintillation bandwidth in the ensemble of measurements. For the above example, with $\langle f_e T \rangle = 5$ in the ensemble of 16 measurements,

estimates of the index had a mean of .95 and an rms deviation from the mean of 0.4, while estimates of f_e varied from 5/T by only 1/T. The gaussian shape of the resultant scintillation spectra obtained over three orders of magnitude in variance density, or three octaves of fluctuation frequency. This supports the statement that constituent (b) discussed in §III is not the result of a smearing of the scintillation spectrum by the transform of the sampling function. The stability of f_e in this experiment is reasonable since with a gaussian spectrum all "lobes" of scintillation have similar widths while their amplitudes have an exponential distribution yielding the greater uncertainty in the index.

IX. DISCUSSION

The pulsar observations discussed in this paper suggest that scintillation indices for point source observations at meter wavelengths are near unity, and that scintillation spectra are gaussian in shape and have a width which scales linearly with dispersion measure. The scatter of individual objects from the spectrum width(f_e)-dispersion measure(DM) trend is a factor of three (fig. 6), and is attributed both to scatter of the mean electron density along various lines of sight (Gómez-Gonzalez and Guélin 1974) and to nonuniformities of the fractional deviation from the mean electron density in different regions of the galaxy. Also, the observations suggest a strong dependence of scintillation index on dispersion measure in the regime of weak scintillation which has been translated to a strong dependence

of the critical radio frequency which separates weak and strong scintillation regimes on dispersion measure. Sutton (1971) has found a similar strong dependence of correlation bandwidth on dispersion measure from a compilation of published data which has been confirmed by the measurements discussed in §V.

In Scheuer's model (1968) and in Salpeter's model (1969) the scintillation bandwidth and correlation bandwidth have the following dependences on velocity of scattering medium transverse to the line of sight (v), thickness of the medium (z), rms density perturbation of thermal electrons on a scale of 10^{11} cm (Δ) and radio frequency (ν) in the strong scattering regime:

$$f_e \propto v\, z^{1/2}\, \Delta\, \nu^{-1}, \text{ and} \tag{8a}$$

$$B_s \propto \nu^4\, z^{-2}\, \Delta^{-2}, \text{ respectively.} \tag{8b}$$

We observe that $f_e \propto DM$ and $B_s \propto DM^{-4}$. If $DM \propto z$, statistically, as argued by Gómez-Gonzalez and Guélin and others, then equation (8) leads immediately to $\Delta \propto z$ and $v \propto z^{-1/2}$ (if $B_s \propto DM^{-3}$, then we could have $\Delta \propto z^{1/2}$ and $v \sim$ constant). On the other hand, if $DM \propto z^{1/2}$, then we could have both v and Δ be independent of DM, and therefore z. Since the HI measurements favor $DM \propto z$, we conclude that the former relations of $\Delta(z)$ and $v(z)$ are closer to the truth. That is, the typical deviation of electron density in the interstellar scattering centers is a growing quantity and the effective pattern speed is

either constant or slowly decreasing with increasing path length in the interstellar medium. A decrease of speed with z is difficult to understand since differential galactic rotation will certainly lead to an increasing speed with distance. This puzzling result suggests the need for firmer estimates of the dependence of f_e and B_s on DM and for more thought on the expected behavior of these quantitives for realistic models of the galaxy.

The explicit formulae for f_e (DM,ν) and ν_c(DM) presented in this paper, and the firm assessment of the shape and normalization of scintillation spectra allow the construction of a model scintillation spectrum for a point source:

$$(9) \qquad P(f) = \left(\frac{2}{\pi f_e^2}\right)^{1/2} \left(1 + \left(\frac{\nu}{\nu_c}\right)^2\right)^{-1} \exp\left(-f^2/2f_e^2\right),$$

where f_e (DM,ν) is given by equation (1) and ν_c (DM) is given by equation (3). The computer modeling of scintillation discussed in §VIII suggests that a single recording of length $T = 5/f_e$ will follow equation (9) with a normalization (scintillation index) error of ≤ 0.4 and width error of $\leq 0.2\ f_e$, where the normalization of unity and width of f_e are ensemble averages of many independent recordings. The observations upon which this paper are based confirm the computer model: when f_eT is small, there are large deviations of normalization and width; when f_eT is large, there are small deviations. Equation (9) can be used to predict the scintillation of a point source of known dispersion measure, and, with the diffraction pattern scale size (eq. 6), to predict the scintillation of an extended source

(Condon and Backer 1974). For example, if the distances to galactic radio stars or molecular line masers are known, then it should be possible to estimate a dispersion measure and consequently to predict an expected scintillation time scale.

The effective pattern speed is the product $2\pi a f_e$, or $50(^{+200}_{-40})$ kms^{-1} for DM = 16 where the bulk of the measurements exist. The above discussion led to a speed dependent on DM^{α} with $0 > \alpha > -1/2$. Consequently the diffraction pattern should scale with DM^{δ} with $-1 > \delta > -1.5$, rather than $\delta = -1/2$ as given in equation 6. Further measurements of a for high dispersion measure pulsars would be useful. Speeds of 50 kms^{-1} are higher than values expected for the transverse components of earth and solar motions with respect to the local standard of rest, random hydrogen cloud velocities and differential galactic rotation over a few hundred parsecs. Some larger speeds either in the medium (Wentzel 1970) or of the pulsar (Gunn and Ostriker 1970, Manchester et al. 1974) must contribute to the phenomenon.

ACKNOWLEDGEMENTS

I would like to thank D.S. Heeschen for the research assistantship which provided the time to perform many of the experiments, my collaborators mentioned in table 1 for their contributions to the experiments, and R. Lovelace for discussions and for the use of his computer program TWINKLE.

REFERENCES

Ables, J.G., Komesaroff, M.M., and Hamilton, P.A. 1970, Astrophys. Letters, 6, 147.

Backer, D.C. 1970a, Nature, 228, 42.

_____. 1970b, ibid, 228, 1297.

_____. 1973, Ap. J., 182, 245.

_____. 1974, ibid, 190, 667.

_____, and Fisher, J.R. 1974, Ap.J., 189, 137.

_____, Rankin, J.M., and Campbell, D.B. 1974, Ap.J., in press.

Cole, T.W., Hesse. K.H., and Page, C.G. 1970, Nature, 225, 712.

Cohen, M.H., and Cronyn, N.M. 1974, Ap.J., 192, 193.

Comella, J.M. 1973, Ph.D. thesis, Cornell University, Ithaca, New York.

Condon, J.J., and Backer. D.C. 1974, Ap.J., in press.

Downs, G.S., and Reichley, P.E. 1971, Ap.J. (Letters), 163, L11.

Gómez-Gonzalez, J., and Guélin, M. 1974, Astron. Astrophys, 32, 441.

Gordon, K.J., and Gordon, C.P. 1973, Astron. Astrophys. 27, 119.

Gunn, J.E., and Ostriker, J.P. 1970, Ap. J., 160, 979.

Hewish, A., Bell, S.J., Pilkington, J.D.H., Scott, P.F., Collins, R.A. 1968, Nature, 217, 709.

Hewish, A. 1970. Ann. Rev. Astron. Astrophys., 8, 265.

Huguenin, G.R., Taylor, J.H., and Troland. T.H. 1970, Ap.J., 162, 727.

_____ and Helfand, D.J. 1973, Ap. J. (Letters), 181, L139.

Lang, K.R. 1969, Ap.J. (Letters), 158, L175.

_____. 1971. Ap.J., 164, 249.

Little, L.T., and Matheson, D.N. 1973, M.N.R.A.S., 162, 329.

Lovelace, R.V.E. 1970, Ph.D. thesis, Cornell University, Ithaca, New York.

_____, and Craft, H.D. 1968, Nature, 220, 875.

_____, and Backer, D.C. 1972, Ap.J.(Letters), 11, 135.

_____. 1974 Paper presented at One Day Meeting on Interstellar Scattering of Radio Waves, JPL, Pasadena, Cal., 1974 February 1.

Manchester, R.N., Taylor, J.H., and Van, Y.Y. 1974, Ap.J. Letters), 189, L119.

McCulloch, P.M., Ables, T.G., Hamilton, P.A., and Komasaroff, M.M. 1974, Nature, in press.

Mutel, R.L., Broderick, J.J., Carr, T.D., Lynch, M., Desch, M., Warnock, W.W., and Klemperer, W.K. 1974, Ap.J., in press.

Prentice, A.J.R., and ter Haar, D. 1969, M.N.R.A.S., 146, 423.

Rankin, J.M., Comella, J.M., Craft, H.D., Richards, D.W., Campbell, D.B., and Counselman, C.C. 1970, Ap. J., 162, 707.

_____, Campbell. D.B., and Backer, D.C. 1974, Ap.J., 188, 609.

Rickett, B.J. 1970, M.N.R.A.S., 150, 67.

Salpeter, E.E. 1969, Nature, 221, 31.

Scheuer, P.A.G. 1968, Nature, 218, 920.

Slee, O.B., Ables, J.G., Batchelor, R.A., Krishna-Mohan, S., Venugopal, V.R., and Swarup, G. 1974, M.N.R.A.S., 167,31.

Sutton, J.M 1971, M.N.R.A.S., 155, 51.

Taylor, J.H., and Huguenin, G.R. 1969, Nature, 221, 816.

_____ , and Hulse, R.A., 1974, IAU Telegram 2704.

Ucsinski, B.J. 1968, Proc. Roy. Soc., A307, 471.

Table 1

Pulsar Observations Containing Interstellar Scintillation

Experiment Goal	Date	Radio Frequency (MHz)	Telescope site-diam.(m)	Radiometer Description	Sample Rate	Time per Source (hr)	Sources	Collaborat
Fluctuation	1972 Apr	250-500	GB-91	250K transistor	$1P_1$	0.7	3	None
Flux density [a]	1972 May	250-500	GB-43	250K transistor	60S	5-8	12	J.R. Fishe
Polarization [b]		1490-8085	GB-26	120K paramps	$1000P_1$			J.M.Rankin
Fluctuation [c]	1971-1974	430	AO-305	150K paramp	$1P_1$	0.5-3	25	D.B.Campbe
Scattering	1972 Oct	408	GB-43, JB-76, AO-305	250K transistor	$1\text{-}5P_1$	5-12	13	A.G. Lyne, G.A. Zeiss
Scattering	1973 Feb	111	GB-91, AO-305	300K transistor	$1P_1$	0.7	5	G.A.Zeissi, N.R.Vanden, T.A. Clark
Scattering [d]	1973 Jun	834	GB-43	200K paramps	$64P_1$	0.5	1	None
	Apr	1667		70K	$128P_1$			
	Jul	4900		100K	$512P_1$			
Flux density	1973 May	250-500	GB-43	250K transistor	60S	5-8	15	J.R. Fishe
		1490-8085	GB-26	120K paramps	$1000P_1$			
Scattering	1974 Feb	1410	GB-43	50K paramp	$1P_1$	0.3	1	M. Ewing
			OV-40	100K paramp				

Table 1 (cont.)

Experiment Goal	Date	Radio Frequency (MHz)	Telescope site - diam.(m)	Radiometer Description	Sample Rate	Time per Source (hr)	Sources	Collaborators
Position	1974 May	2695	GB-26	120K paramps	0.3 hr	4	5	R.A. Sramek
Flux density	1974 May	775/968 1440	GB-91	150K 50K	paramps 48 hr	0.1	53	J.R. Fisher

[a] see Backer and Fisher (1974)

[b] see Rankin, Campbell and Backer (1974)

[c] see Backer, Rankin and Campbell (1974)

[d] see Backer (1974)

Table 2
400 MHz Scintillation Spectra

PSR	P (s)	DM ($pc\text{-}cm^{-3}$)	BW (MHz)	NxM (P_1)	m	f_e (mHz)	f_t (mHz)	f_eT	Data
0031-07	0.943	10.9	3.0	1,024x1	0.80	1.3	1.5	1	GBFF
0301+19	1.388	15.7	0.5	8,192x1	0.90	0.88	1.64	10	JBIS
0329+54	0.715	26.8	0.5	16,384x3	0.55	1.48	2.80	19	JBIS
0525+21	3.745	50.8	2.0	1,024x1	0.92	12.5	13.0	52	AOPN
0540+23	0.246	72.	0.1	4,096x1	0.35	27.8	52.0	28	AOPN
0611+22	0.335	96.7	0.1	4,096x1	0.30	5.1	7.0	24	AOPN
0809+74	1.292	5.7	3.0	2,048x1	1.00	0.8	3.0	1	GBFF
0823+26	0.531	19.4	0.5	32,768x1	0.95	1.85	4.70	30	GBIS
0834+06	1.274	12.9	2.0	16,384x1	0.75	0.86	2.00	6	JBIS
0943+10	1.098	15.4	2.0	1,024x1	0.55	3.55	5.30[a]	4	AOPN
0950+08	0.253	3.0	2.0	8,192x5	1.15	0.19	0.45	2	JBIS
1133+16	1.188	4.8	2.0	8,192x1	1.07	1.30	2.60	17	JBIS
1237+25	1.382	9.3	2.0	2,048x1	1.00	0.70	1.75	2	AOPN
1508+55	0.740	19.6	0.5	16,384x1	0.30	4.30	5.00[a]	52	JBIS
1541+09	0.748	35.0	2.0	2,048x1	$\leq$0.05	$\leq$0.65	-	-	AOPN
1604-00	0.422	10.7	2.0	2,048x1	$\leq$0.10	$\leq$1.15	-	1	AOPN
1642-03	0.388	35.7	0.5	32,768x1	0.60	3.75	7.00	48	JBIS
1915+13	0.195	94.	0.1	2,048x1	0.20	5.00	6.30[a]	2	AOPN
1919+21	1.337	12.4	2.0	8,192x1	1.23	0.64	2.00	7	GBIS
1929+10	0.227	3.2	2.0	16,384x1	1.65	1.07	1.25	4	JBIS
1933+16	0.359	158.5	0.1	1,024x1	0.08	8.20	8.20	3	AOPN
1944+17	0.441	16.3	2.0	2,048x1	-	$\leq$1.0	-	-	AOPN
2016+28	0.558	14.2	0.5	16,384x3	0.75	0.58	0.55	16	JBIS
2020+28	0.343	24.6	0.5	2,048x1	0.90	2.85	6.80	3	AOPN

Table 2 (cont)

PSR	P (s)	DM (pc-cm^{-3})	BW (MHz)	NxM (P_1)	m	f_e (mHz)	f_t (mHz)	f_eT	Data
2021+51	0.529	22.6	0.5	16,384x1	0.75	0.69	1.85	6	JBIS
2045-16	1.962	11.5	2.0	4,096x1	1.65	(1.00)	1.57	11	JBIS
2217+47	0.538	43.5	0.5	16,384x3	0.35	2.12	4.10[a]	56	JBIS
2303+30	1.576	49.9	2.0	2,048x1	$\leq$0.37	(3.10)	(3.0)	1	AOPN

[a]Values may be limited by receiver noise rather than by intrinsic fluctuations as discussed in text.

Table 3

SCINTILLATION PARAMETERS AT 2695 MHz

PSR	μ	f_e (mHz)	$f_e T$	Data
0329+54	0.38	0.23	4.5	A
	0.90	-	-	B
0355+54	0.38[a]	0.58	4.5	A
0628-28	0.69	0.12	2.5	A
0823+26	0.94	0.32	8.5	A
0833-45	0.10[a]	-	-	A
0950+08	$\leq$0.10	-	-	A
	0.22	-	-	B
1133+16	0.24	0.24	6	A
	0.52	-	-	B
1237+25	0.35	0.36	8	A
1706-16	0.45	0.35	5.5	A
1749-28	1.05	0.14	2	A
1929+10	0.53	0.18	4	A
	0.52	-	-	B
1933+16	0.20[a]	0.25	6	A
2016+28	$\geq$0.67	0.05	$\leq$1	A
2021+51	0.70	0.10	2.5	A
	0.84	-	-	B

[a]Suppressed from ~1.0 by 60-MHz bandwidth.

FIGURE CAPTIONS

Fig. 1 Schematic spectrum of pulsar fluctuations with four regions (a-d) identified which are discussed in the text.

Fig. 2 Normalized variance-density spectrum for PSR 0329+54. Upper abscissa scale is for the high-resolution spectrum (solid) and lower abscissa scale is for the low-resolution spectrum (dashed). A gaussian curve (dash-dotted) is drawn through the low-frequency end of the high-resolution spectrum.

Fig. 3 Normalized variance-denstiy spectrum for PSR 0823+26. Upper abscissa scale is for the high-resolution spectrum (solid) from 408-MHz data and lower abscissa scale is for the low-resolution spectrum (dashed) of 430-MHz data. A gaussian curve (dash-dotted) is drawn through the low-frequency end of the high-resolution spectrum.

Fig. 4 Normalized variance-density spectrum for PSR 1133+16. See caption to fig. 2 for further details.

Fig. 5 Normalized variance-density spectra for PSR's 0329+54 (a), 0823+26 (b), and 1133+16 (c) from 2695-MHz data. The scales are identical to those of figures 2 to 4, respectively.

Fig. 6 Scintillation bandwidths of pulsars near 400 MHz. Upper limits are shown for three objects with arrowed points. The point outside the dotted lines at DM = 70 pc cm^{-3} is for the Vela pulsar.

Fig. 7 Scintillation indices of pulsars at 2695 MHz from observations of the author and from published data of Downs and Reichley (1971)

Fig. 8 Radio-frequency dependence of scintillation index estimates for nine pulsars.

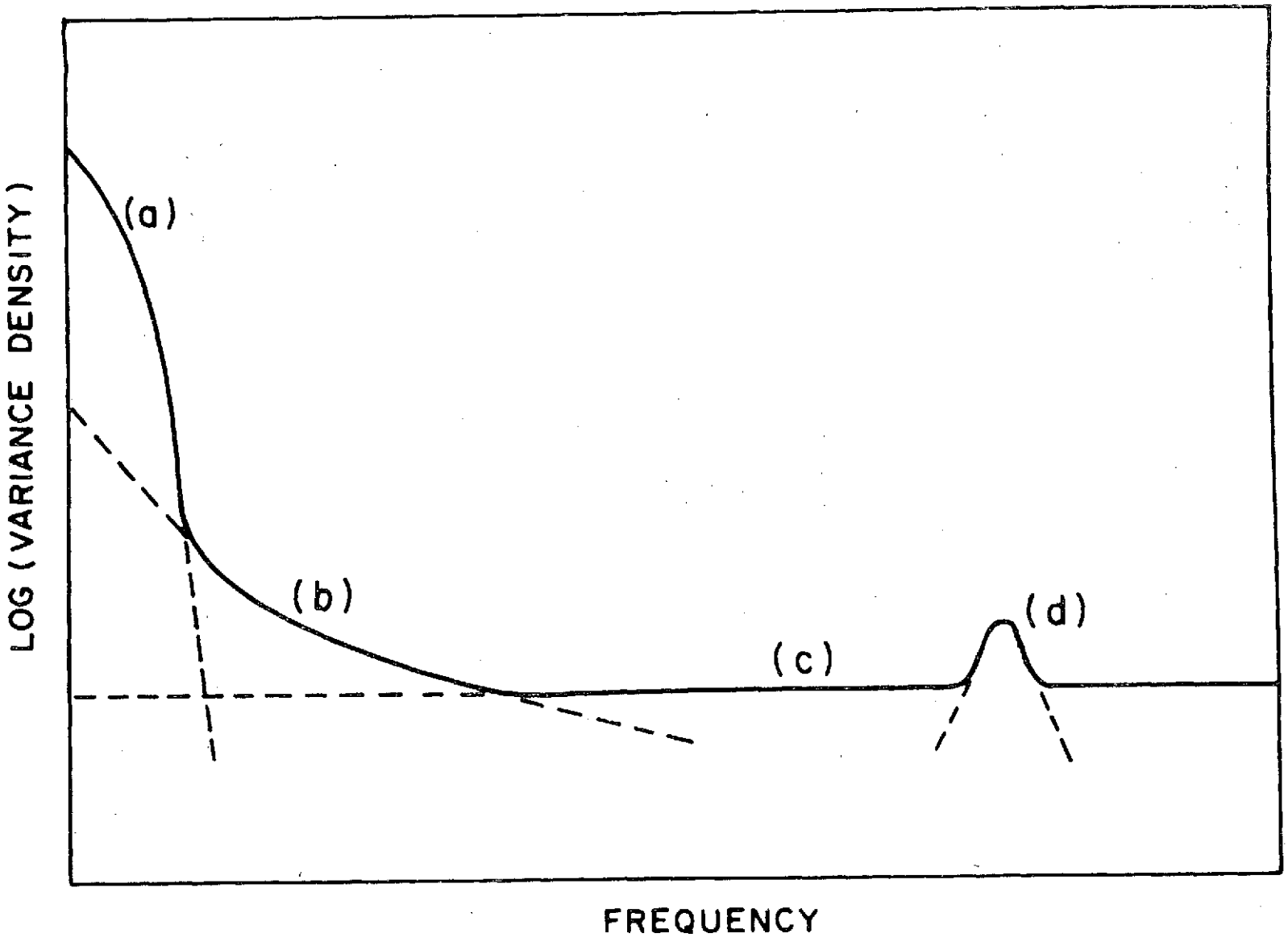

FIGURE 1

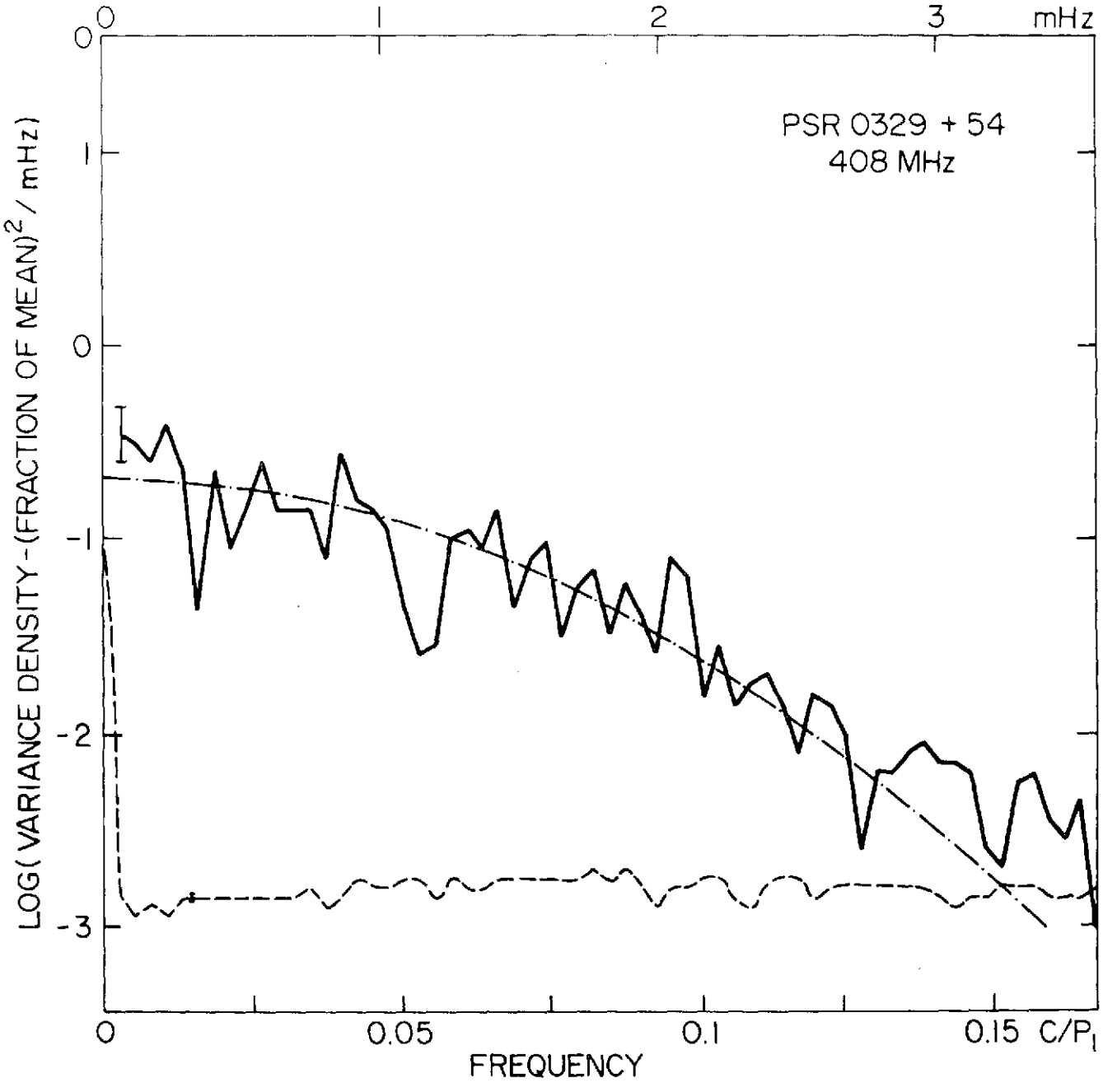
0
1
2
3
mHz
PSR 0329 + 54
408 MHz
LOG(VARIANCE DENSITY - (FRACTION OF MEAN)^2 / mHz)
0
-1
-2
-3
0
0.05
0.1
0.15 C/P$_1$
FREQUENCY

FIGURE 2

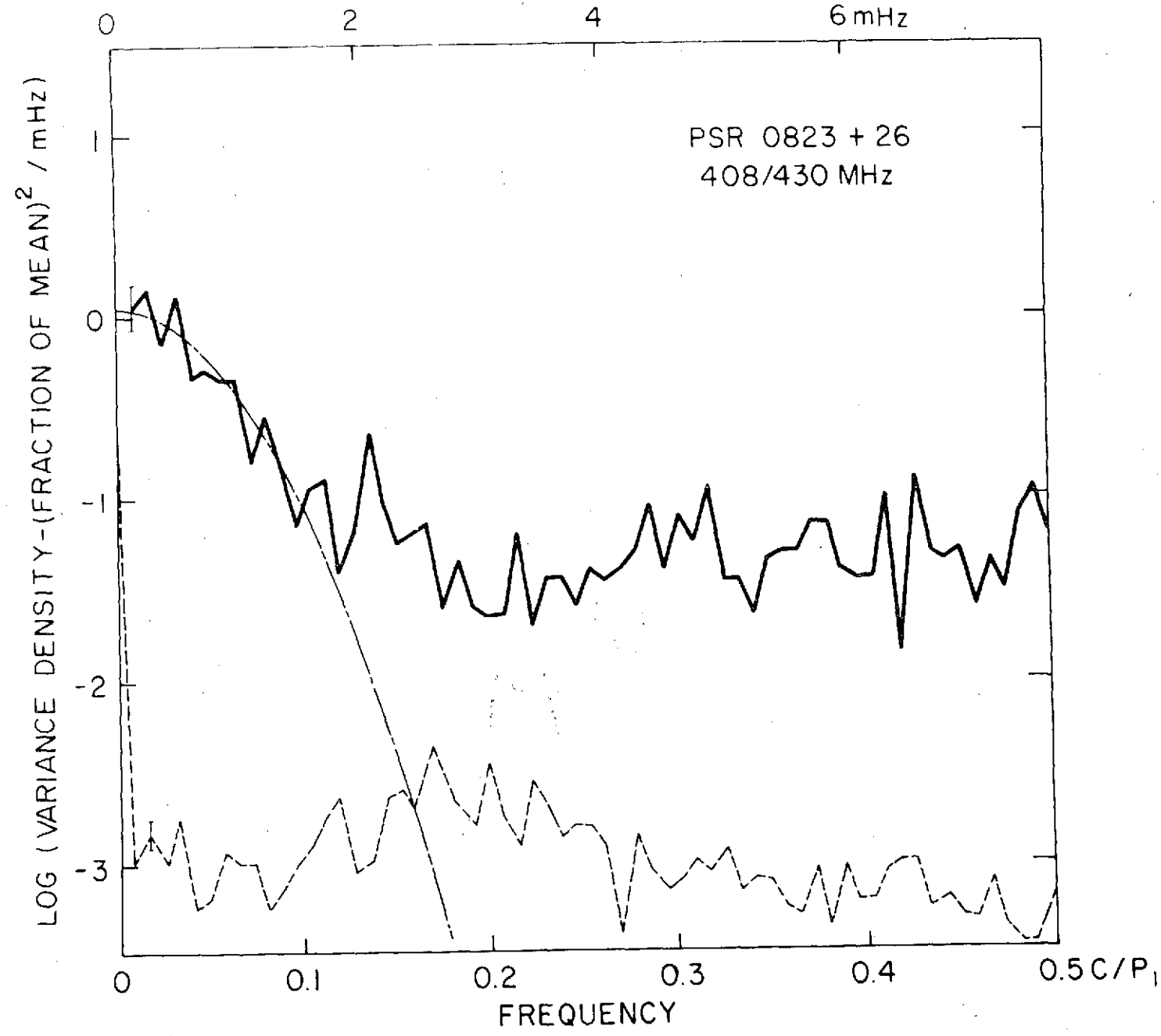
0
2
4
6 mHz
PSR 0823 + 26
408/430 MHz
LOG (VARIANCE DENSITY-(FRACTION OF MEAN)^2 / mHz)
1
0
-1
-2
-3
0
0.1
0.2
0.3
0.4
0.5 C/P$_1$
FREQUENCY

FIGURE 3

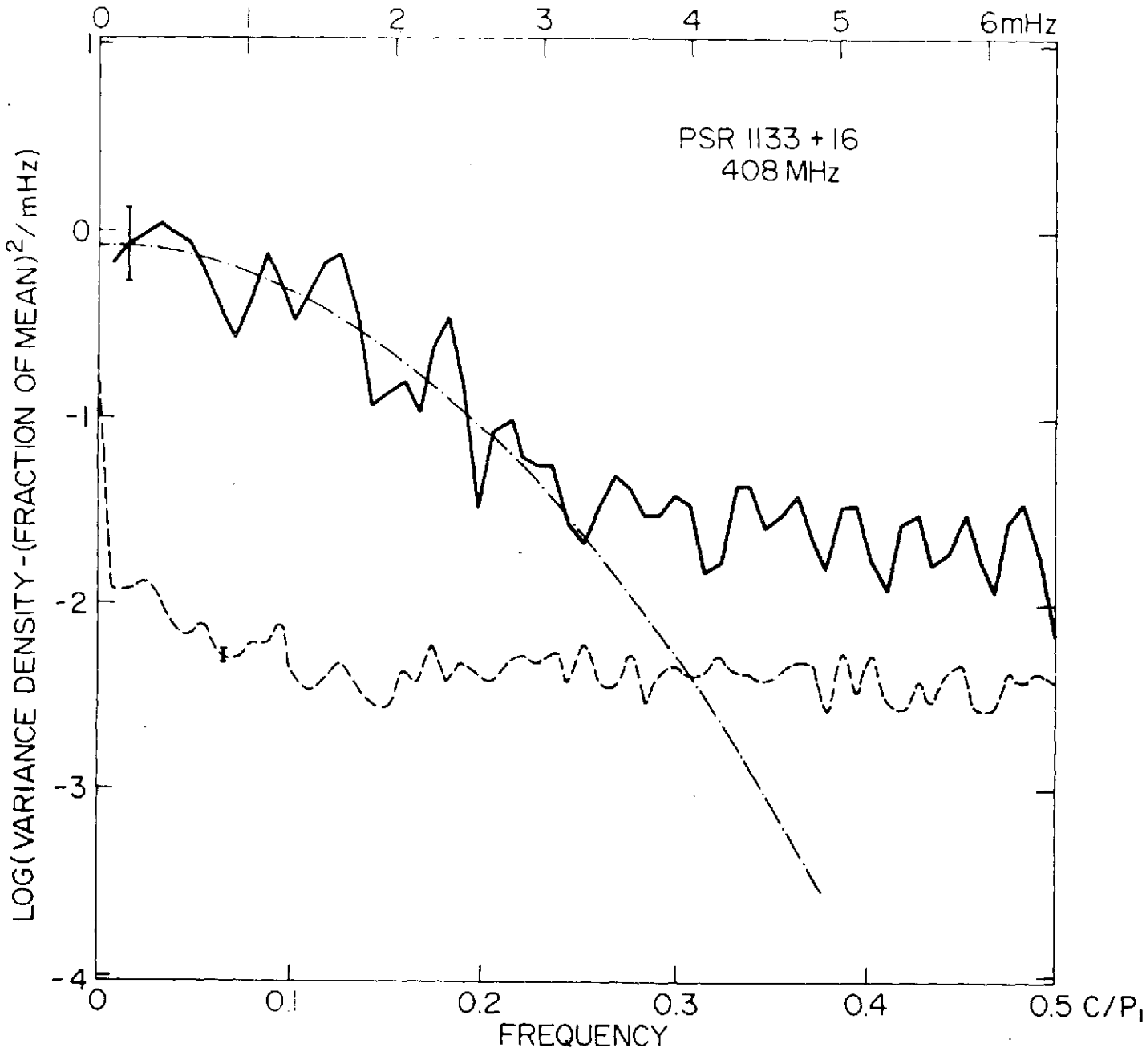
0
1
2
3
4
5
6mHz
PSR 1133 + 16
408 MHz
LOG(VARIANCE DENSITY-(FRACTION OF MEAN)²/mHz)
0
-1
-2
-3
-4
0
0.1
0.2
0.3
0.4
0.5 C/P₁
FREQUENCY

FIGURE 4

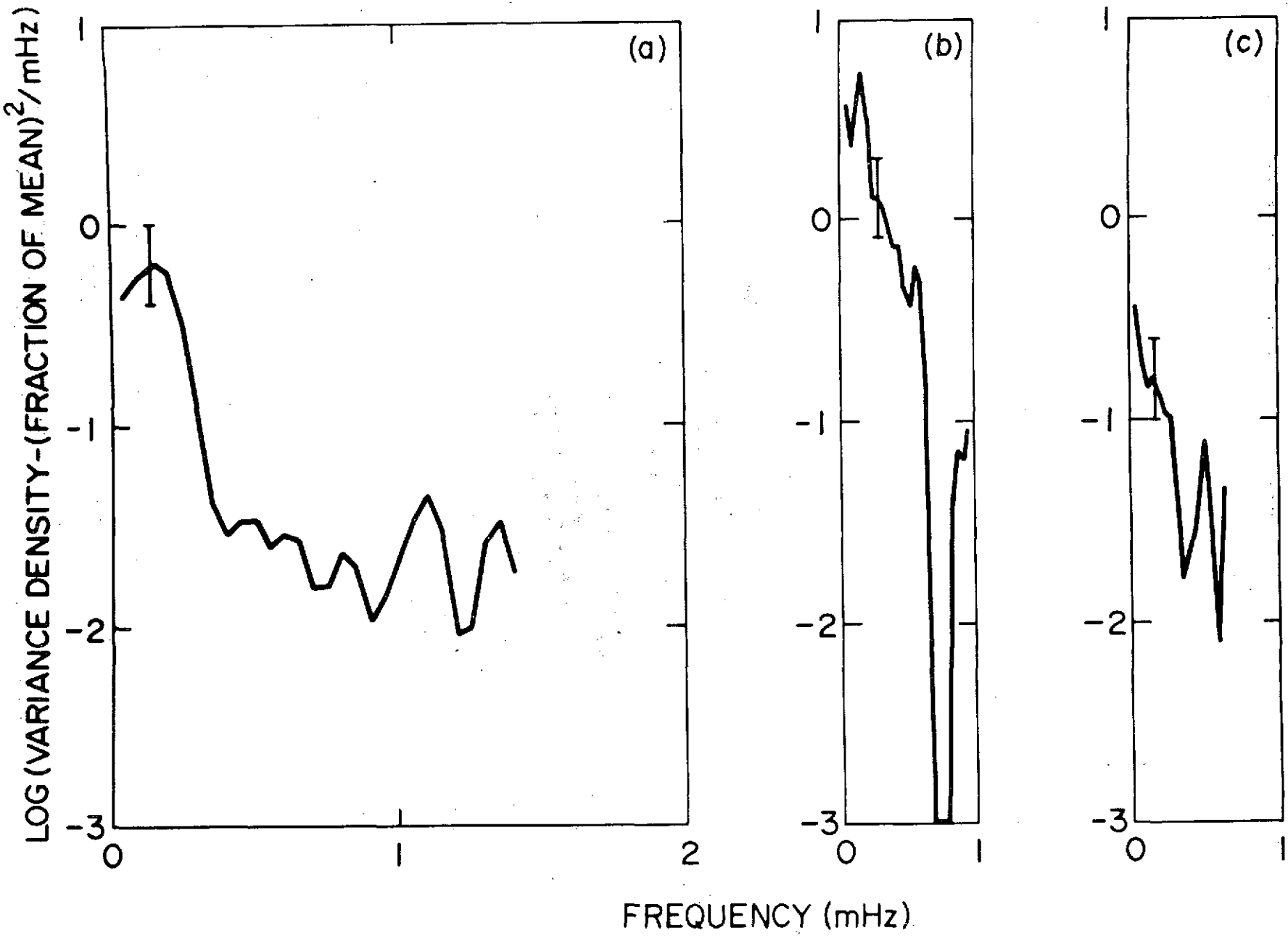
LOG (VARIANCE DENSITY-(FRACTION OF MEAN)^2/mHz)
(a)
(b)
(c)
1
0
-1
-2
-3
0
1
2
FREQUENCY (mHz)

FIGURE 5

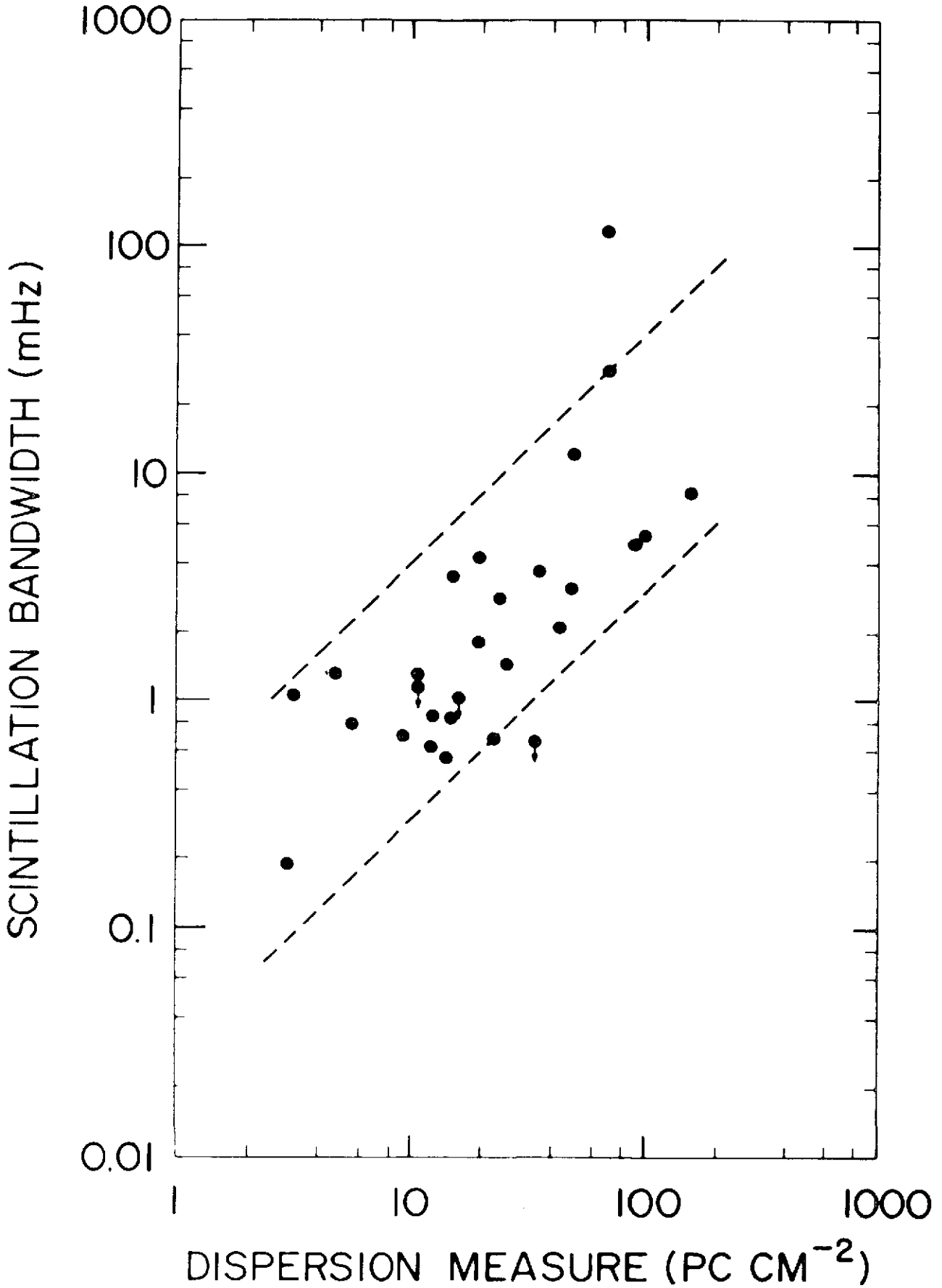
1000
100
10
1
0.1
0.01
SCINTILLATION BANDWIDTH (mHz)
1
10
100
1000
DISPERSION MEASURE (PC CM^{-2})

FIGURE 6

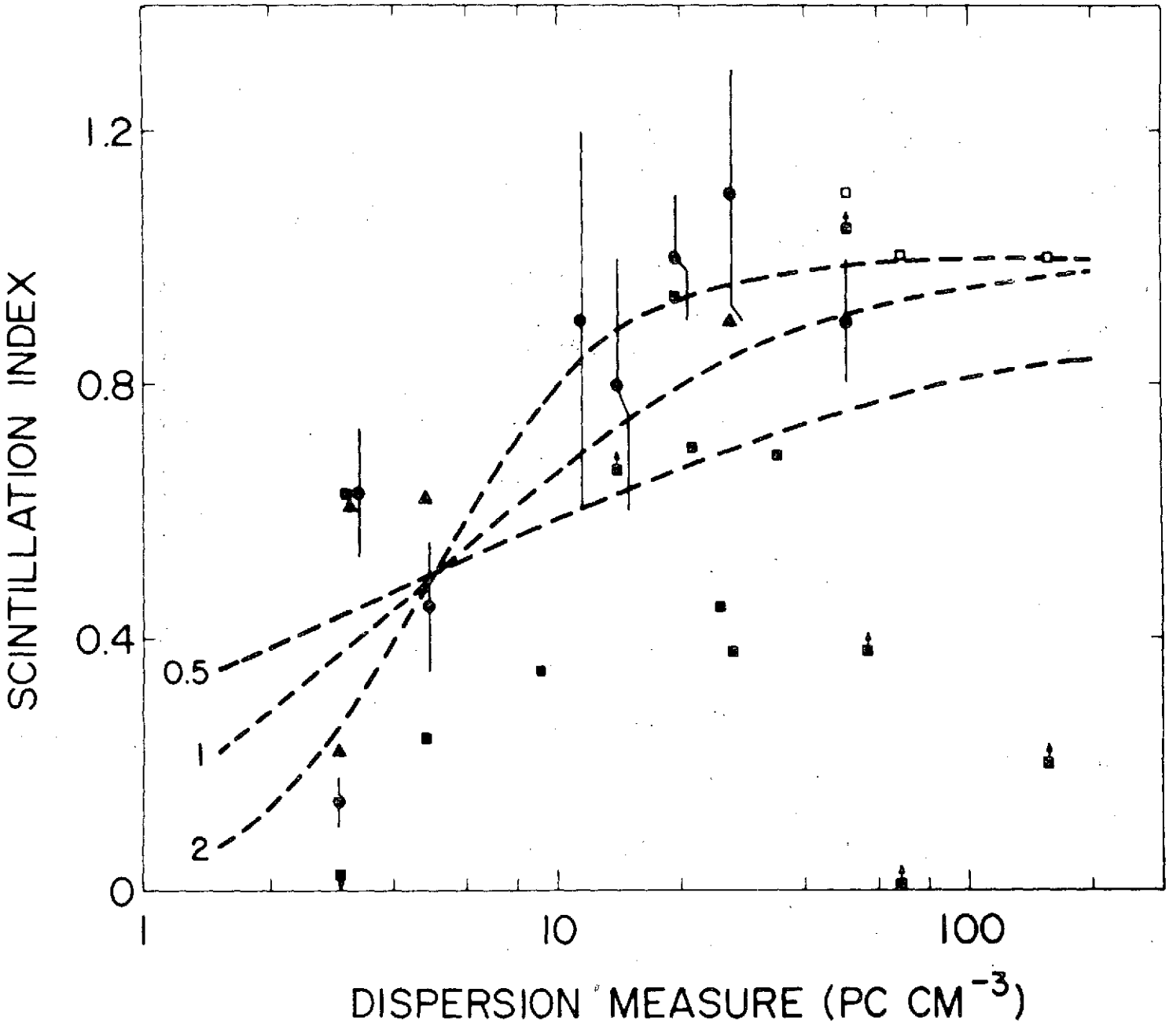
SCINTILLATION INDEX
1.2
0.8
0.4
0
0.5
1
2
1
10
100
DISPERSION MEASURE (PC CM^{-3})

FIGURE 7

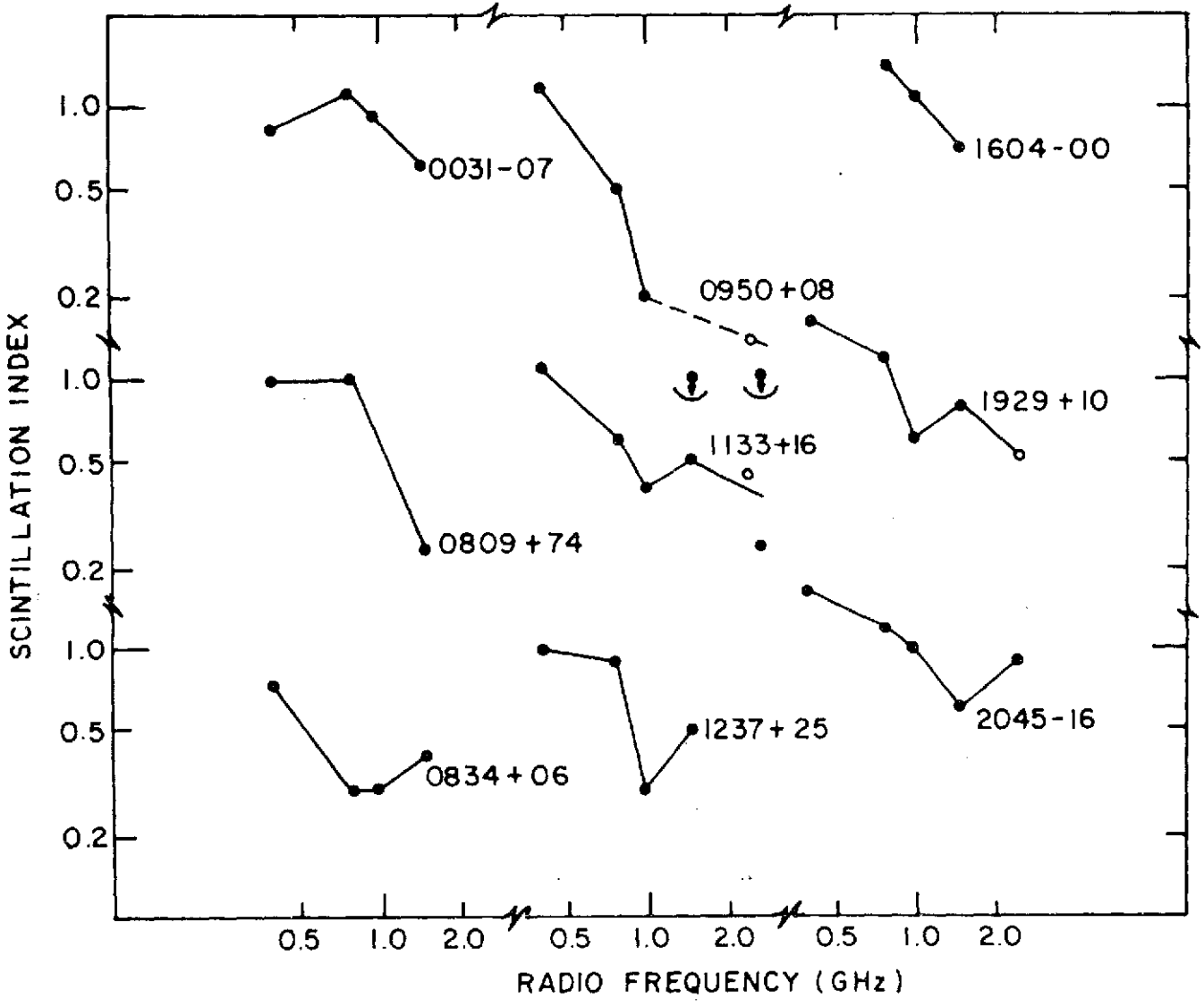
SCINTILLATION INDEX
1.0
0.5
0.2
1.0
0.5
0.2
1.0
0.5
0.2
0031-07
1604-00
0950+08
1929+10
1133+16
0809+74
2045-16
1237+25
0834+06
0.5
1.0
2.0
0.5
1.0
2.0
0.5
1.0
2.0
RADIO FREQUENCY (GHz)

FIGURE 8

APPENDIX I*

VARIANCE-DENSITY SPECTRA FOR 28 PULSARS

In §§III and IV of this paper we discuss the shapes of the scintillation portion of normalized, variance-density spectra (VDS's) observed for pulsars near 400 MHz and relate the width of these functions to the dispersion measures, or column density of interstellar thermal electrons. In this prepublication document we present the VDS's for 28 pulsars upon which the discussion in §III and the measurements in §IV are based.

For most objects a high-resolution VDF(solid line and upper frequency scale) and a low-resolution VDS (dashed line and lower frequency scale) are given on a semilogarithmic grid in the following pages. The low-resolution frequencies are in units of cycles per pulse period (c/P_1). The pulsar designation and observing frequency (-ies) are noted in the upper righthand corner of each plot. When two frequencies are given, the first (408 MHz) refers to the high-resolution VDS and the second (430 MHz) refers to the low-resolution VDS. This division occurs since the 408-MHz data are of longer extent, allowing higher resolution and a more nearly stationary VDS, while the 430-MHz data have superior sensitivity,

*The following pages will not be submitted for publication.

revealing the short-term fluctuations in cases of weak signals. In these cases the high-resolution spectrum typically decays to a level of the system noise in the 408-MHz observations (e.g., see PSR 0823+26).

Error bars are given for both VDS's based on the number of degrees of freedom in the plotted points: two, for the sine and cosine components in the raw VDS, times n for the smoothing performed before plotting. The error was taken to be a factor of $(2\ n)^{1/2}$. For a stationary random signal, such as the typical system fluctuations, this error should give the standard deviation of the points of a VDS from the (local) mean. In many cases we have not obtained sufficient data to provide a stationary estimate of the scintillation portions of the VDS's. This is discussed in more detail in §§III and VIII. On the other hand, it is found that the low-resolution VDS's do provide stationary estimates of the fluctuations intrinsic to the pulsar emission. Deviations in the low-resolution VDS's from a "white" continuum which are significant relative to the errors are related to periodic subpulse variations (e.g., see PSR 0823+26), or to bursts of emission (e.g., see PSR 1944+17); these

deviations are discussed in more detail by Backer, Rankin and Campbell (1974).

A third curve (dash-dotted line) is given which is a subjective fit of a half-gaussian to the scintillation portion of the high-resolution VDS, when it can be identified, as discussed in §III. In most cases the VDS follows a gaussian curve within the quoted statistical errors. A further constraint on the fitting was that the area of the gaussian be near unity. This fact explains why a poor "fit" is given for PSR 1919+21. It was felt that since unity for scintillation indices is appropriate in most objects, it is probably appropriate for all objects. The "excess" variance-density at scintillation-like frequencies then would be due to variations intrinsic to the pulsar. This hypothesis could be tested by simultaneously inspecting the correlation bandwidth of the fluctuations to determine what fraction of the fluctuations is due to the (narrow-bandwidth) scintillation. This experiment would be useful for all objects listed in table 2 with large estimated scintillation indices.

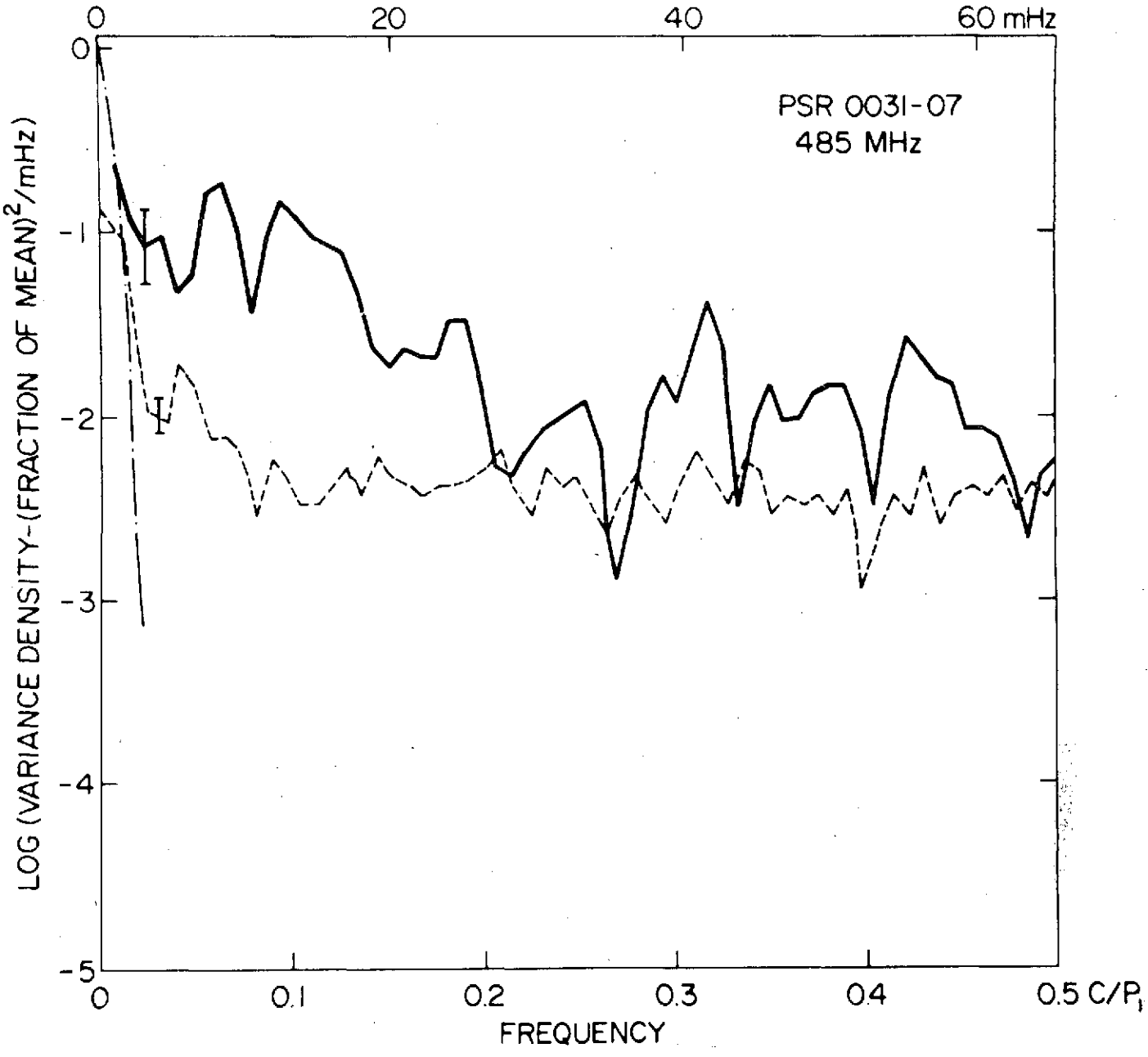
0
20
40
60 mHz
PSR 0031-07
485 MHz
LOG (VARIANCE DENSITY-(FRACTION OF MEAN)²/mHz)
0
-1
-2
-3
-4
-5
0
0.1
0.2
0.3
0.4
0.5 C/P₁
FREQUENCY

1

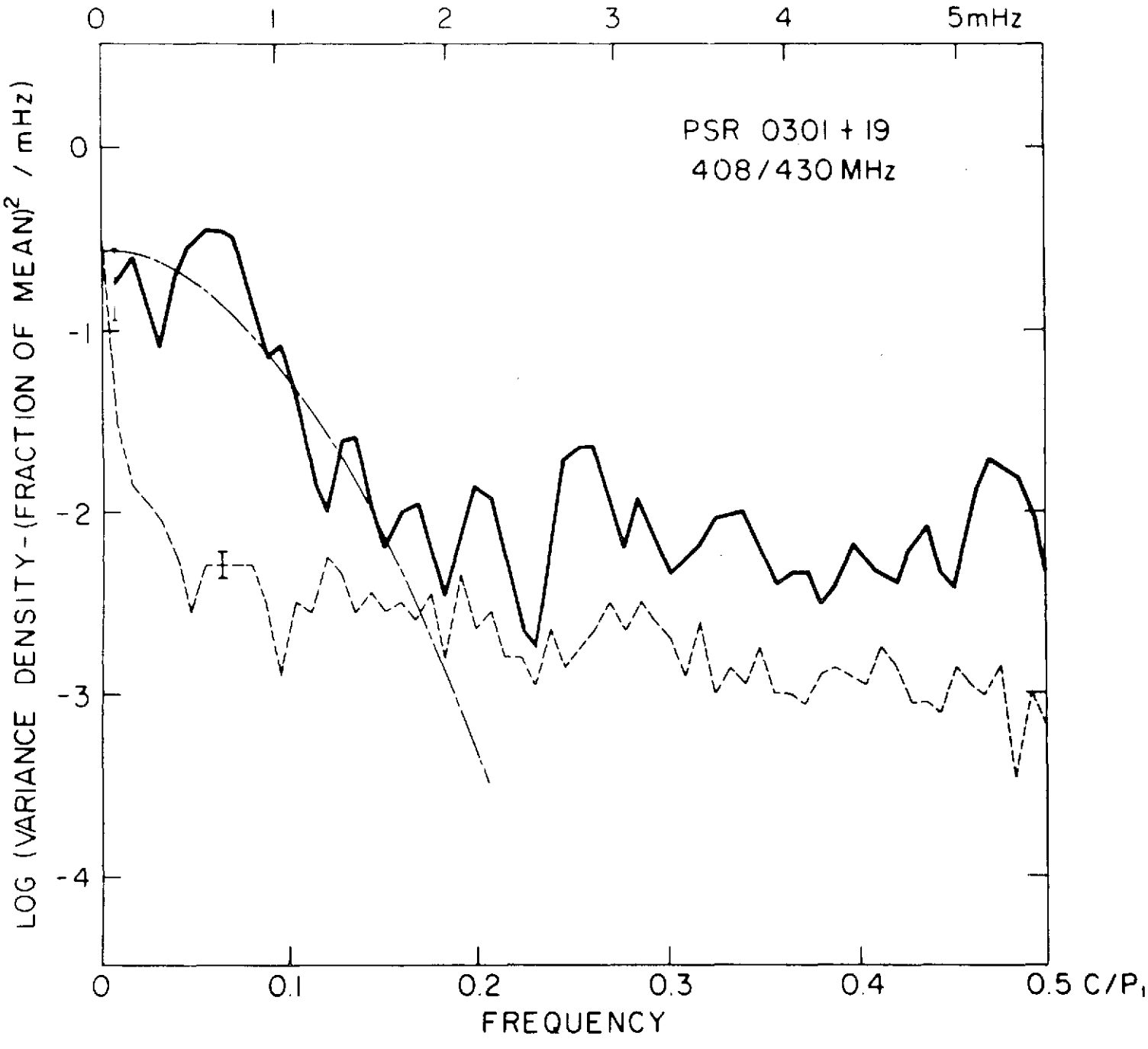
0
1
2
3
4
5mHz
PSR 0301 + 19
408/430 MHz
LOG (VARIANCE DENSITY-(FRACTION OF MEAN)² / mHz)
0
-1
-2
-3
-4
0
0.1
0.2
0.3
0.4
0.5 C/P₁
FREQUENCY

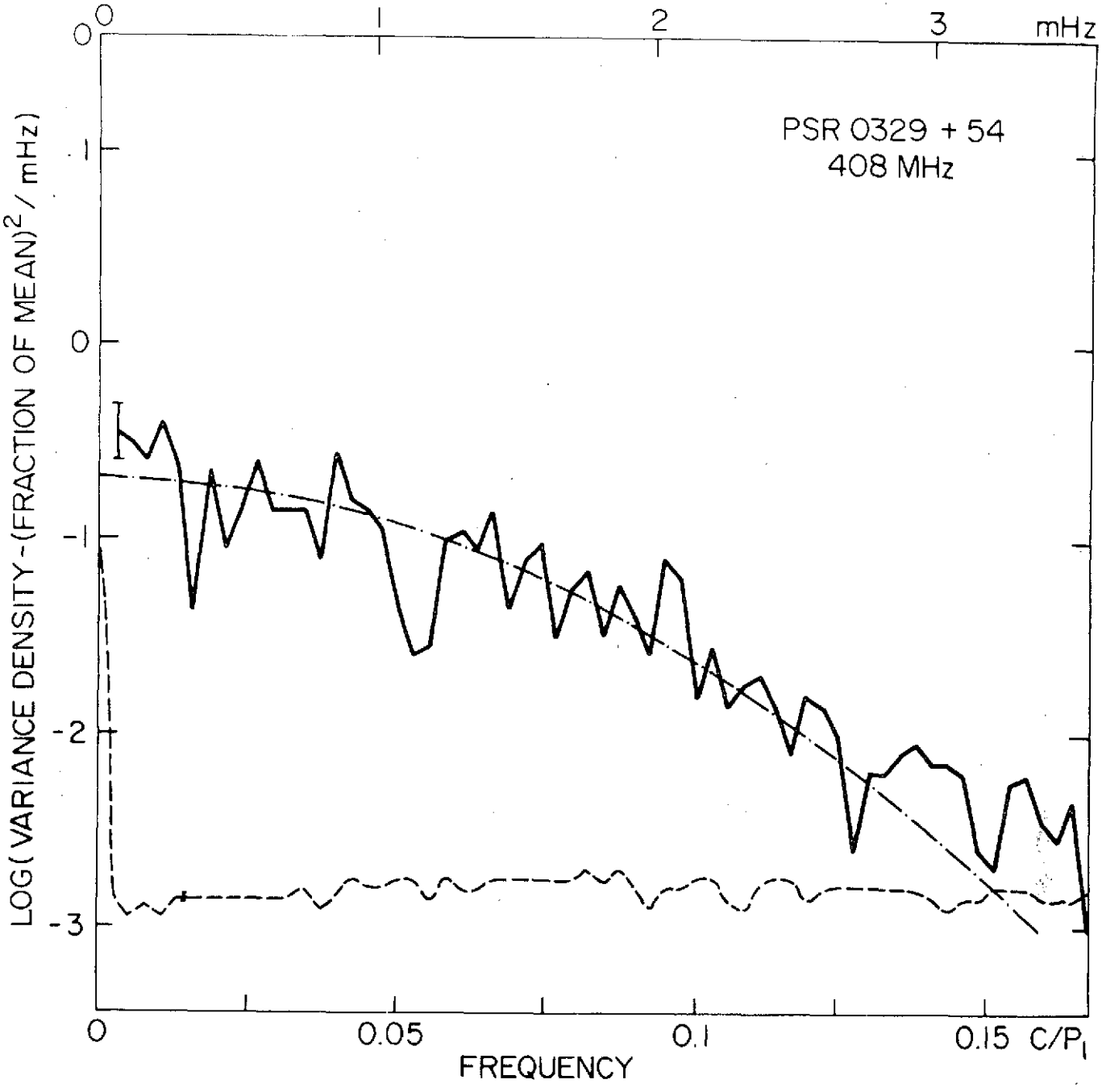
0
1
2
3
mHz
PSR 0329 + 54
408 MHz
LOG(VARIANCE DENSITY - (FRACTION OF MEAN)^2 / mHz)
0
-1
-2
-3
0
0.05
0.1
0.15 C/P$_1$
FREQUENCY

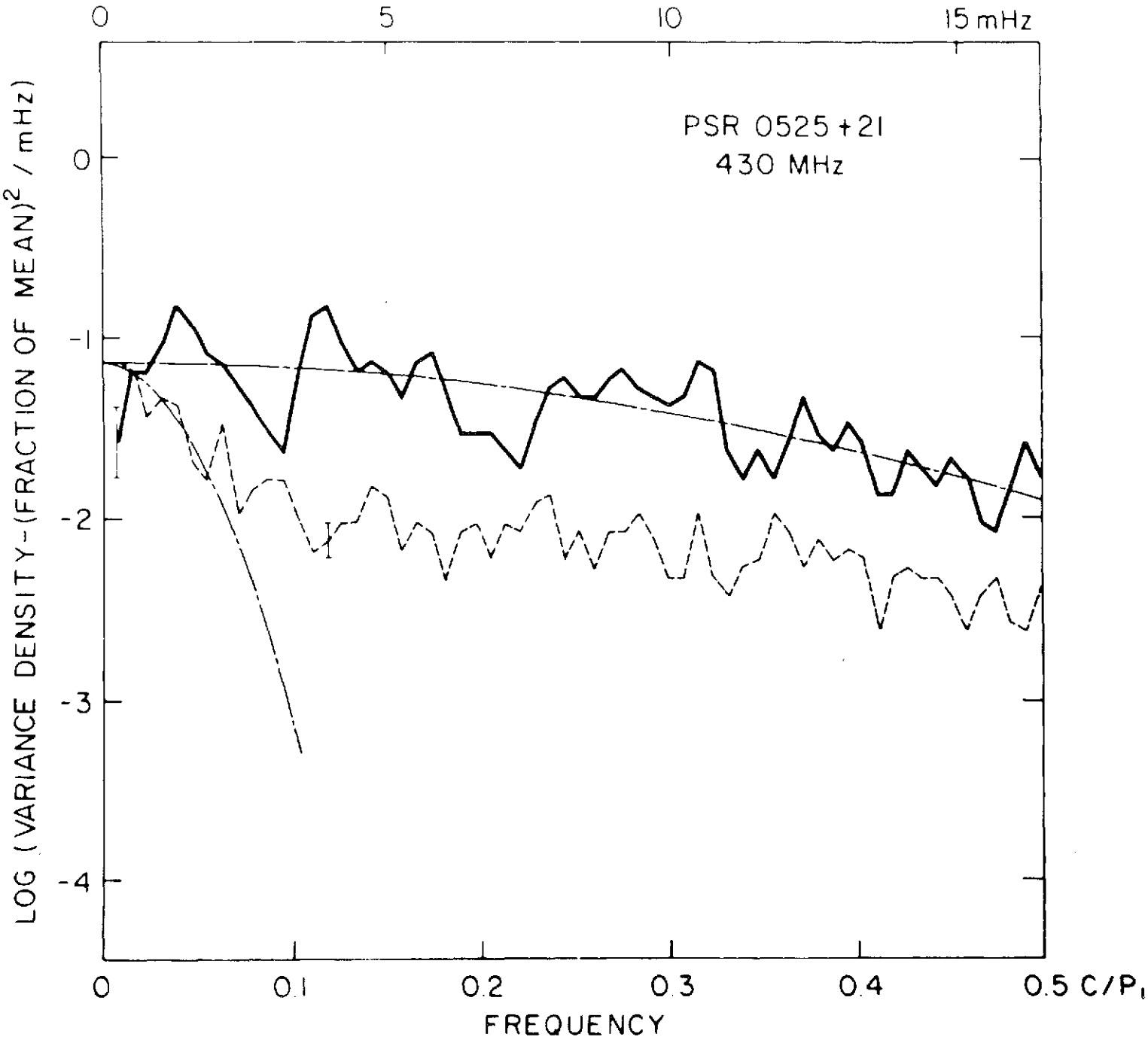
0
5
10
15 mHz
PSR 0525+21
430 MHz
LOG (VARIANCE DENSITY-(FRACTION OF MEAN)^2 / mHz)
0
-1
-2
-3
-4
0
0.1
0.2
0.3
0.4
0.5 C/P$_1$
FREQUENCY

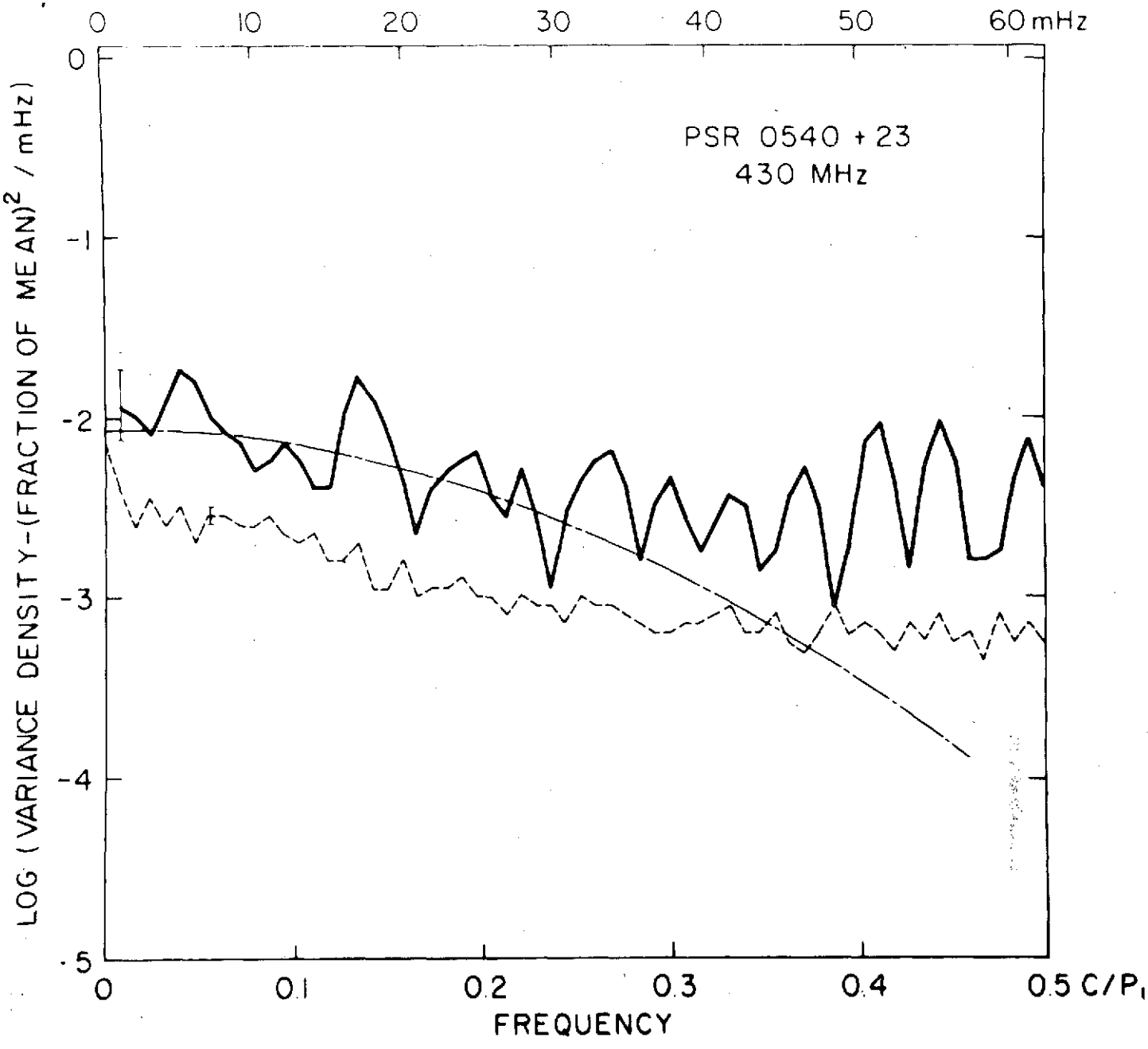
0
10
20
30
40
50
60 mHz
PSR 0540 + 23
430 MHz
LOG (VARIANCE DENSITY-(FRACTION OF MEAN)^2 / mHz)
0
-1
-2
-3
-4
-5
0
0.1
0.2
0.3
0.4
0.5 C/P$_1$
FREQUENCY

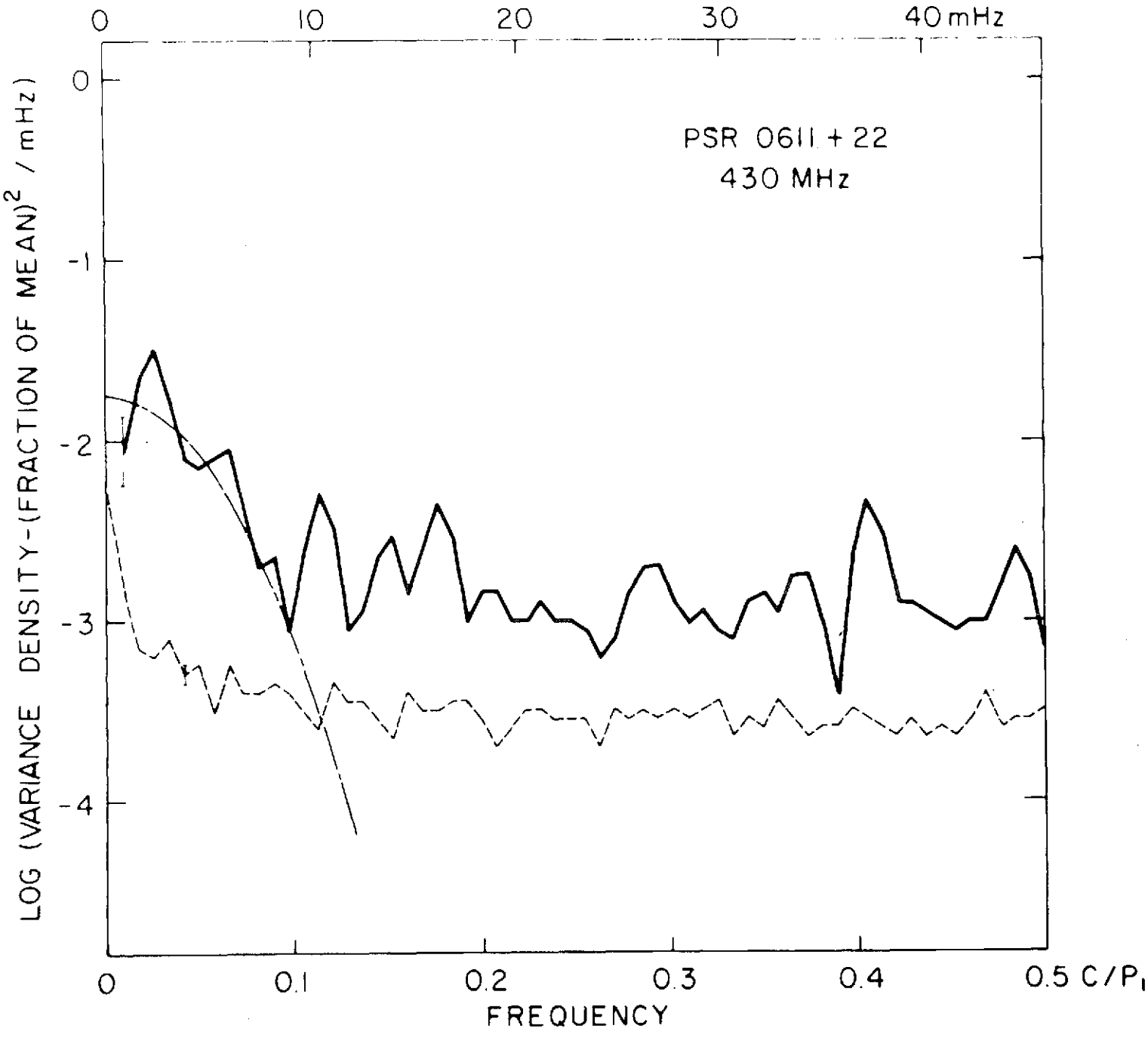
0
10
20
30
40 mHz
PSR 0611 + 22
430 MHz
LOG (VARIANCE DENSITY-(FRACTION OF MEAN)^2 / mHz)
0
-1
-2
-3
-4
0
0.1
0.2
0.3
0.4
0.5 C/P$_1$
FREQUENCY

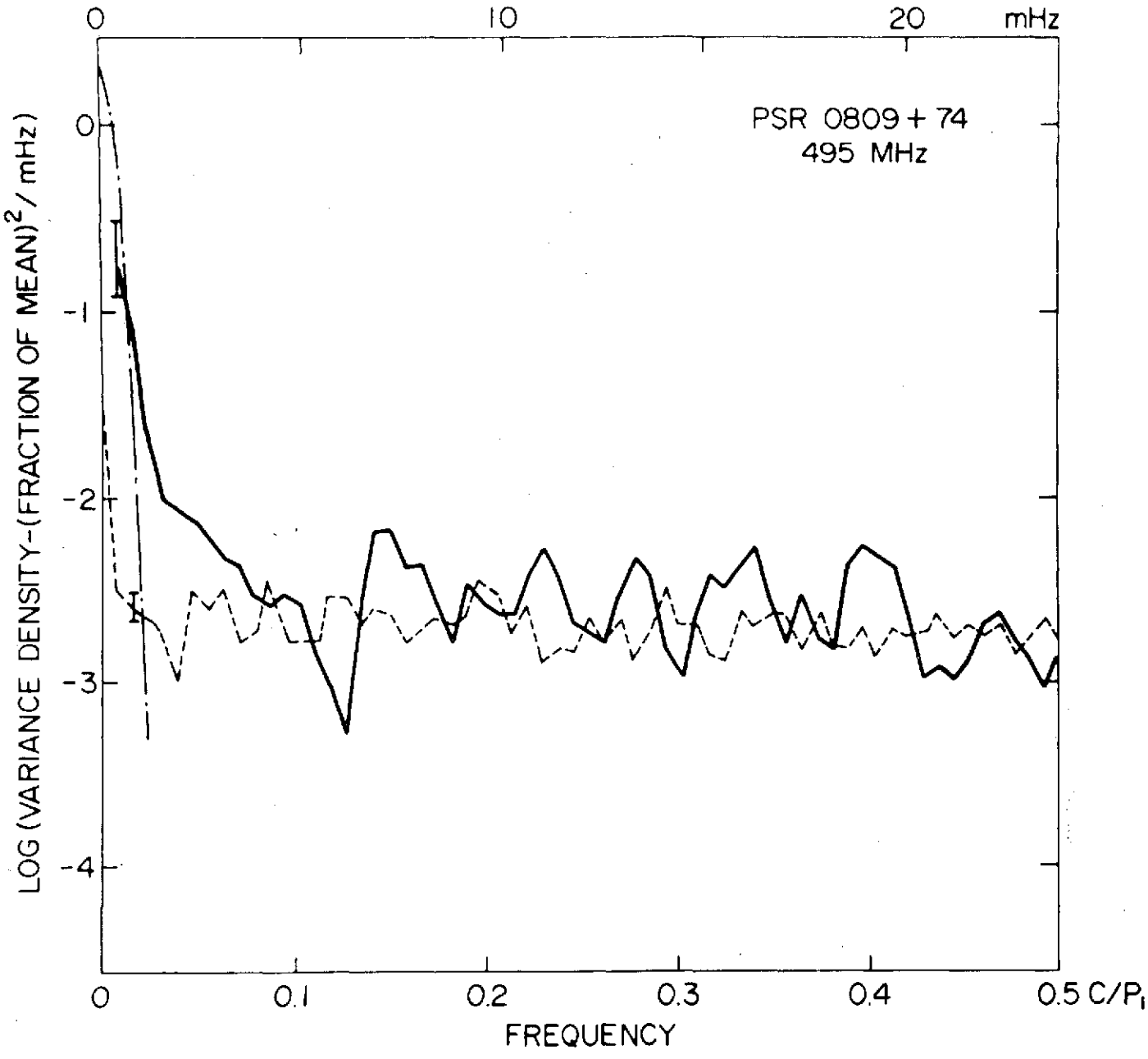
0
10
20
mHz
PSR 0809 + 74
495 MHz
LOG (VARIANCE DENSITY-(FRACTION OF MEAN)^2/ mHz)
0
-1
-2
-3
-4
0
0.1
0.2
0.3
0.4
0.5 C/P$_1$
FREQUENCY

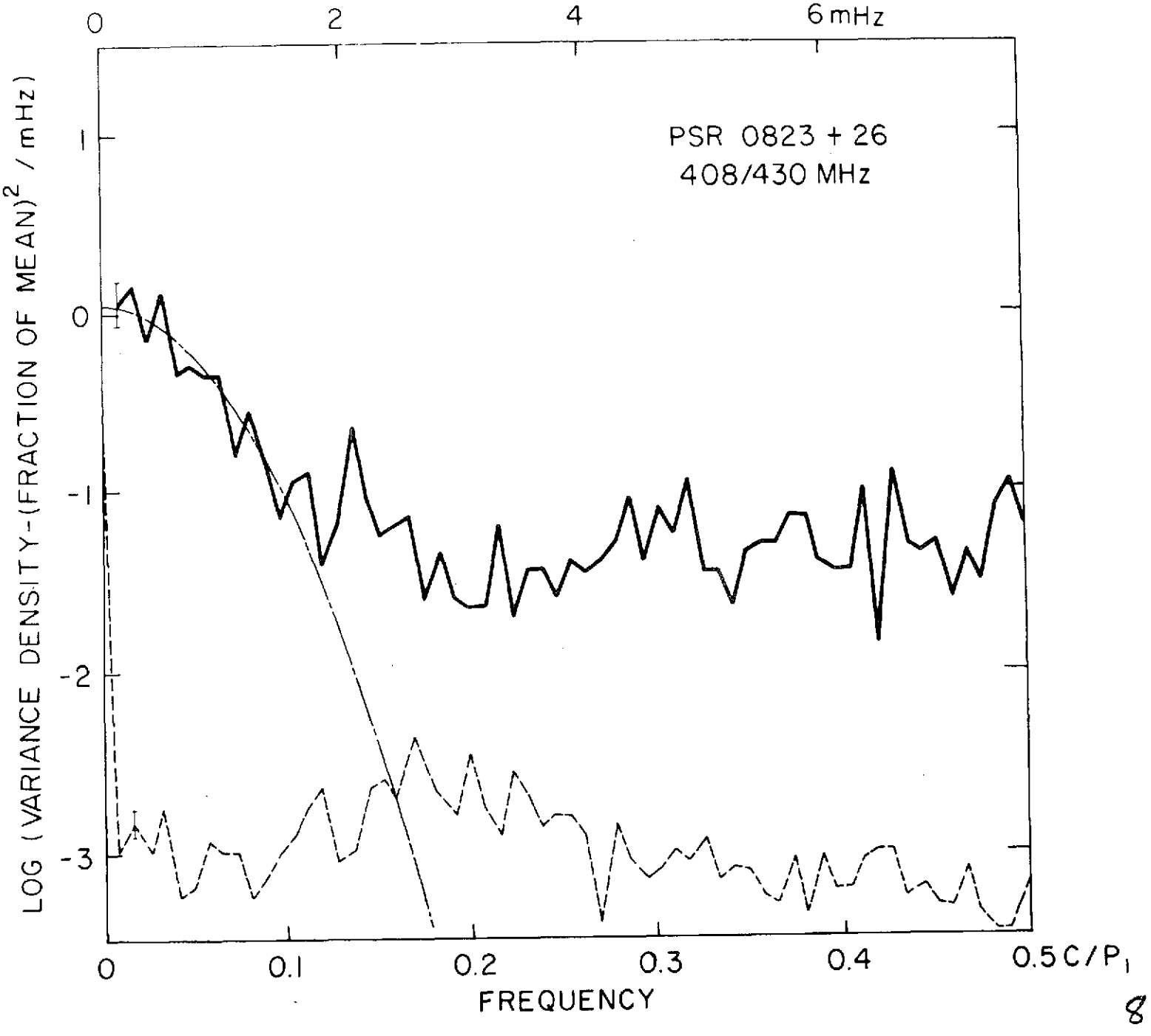
0
2
4
6 mHz
PSR 0823 + 26
408/430 MHz
LOG (VARIANCE DENSITY-(FRACTION OF MEAN)^2 / mHz)
1
0
-1
-2
-3
0
0.1
0.2
0.3
0.4
0.5 C/P$_1$
FREQUENCY

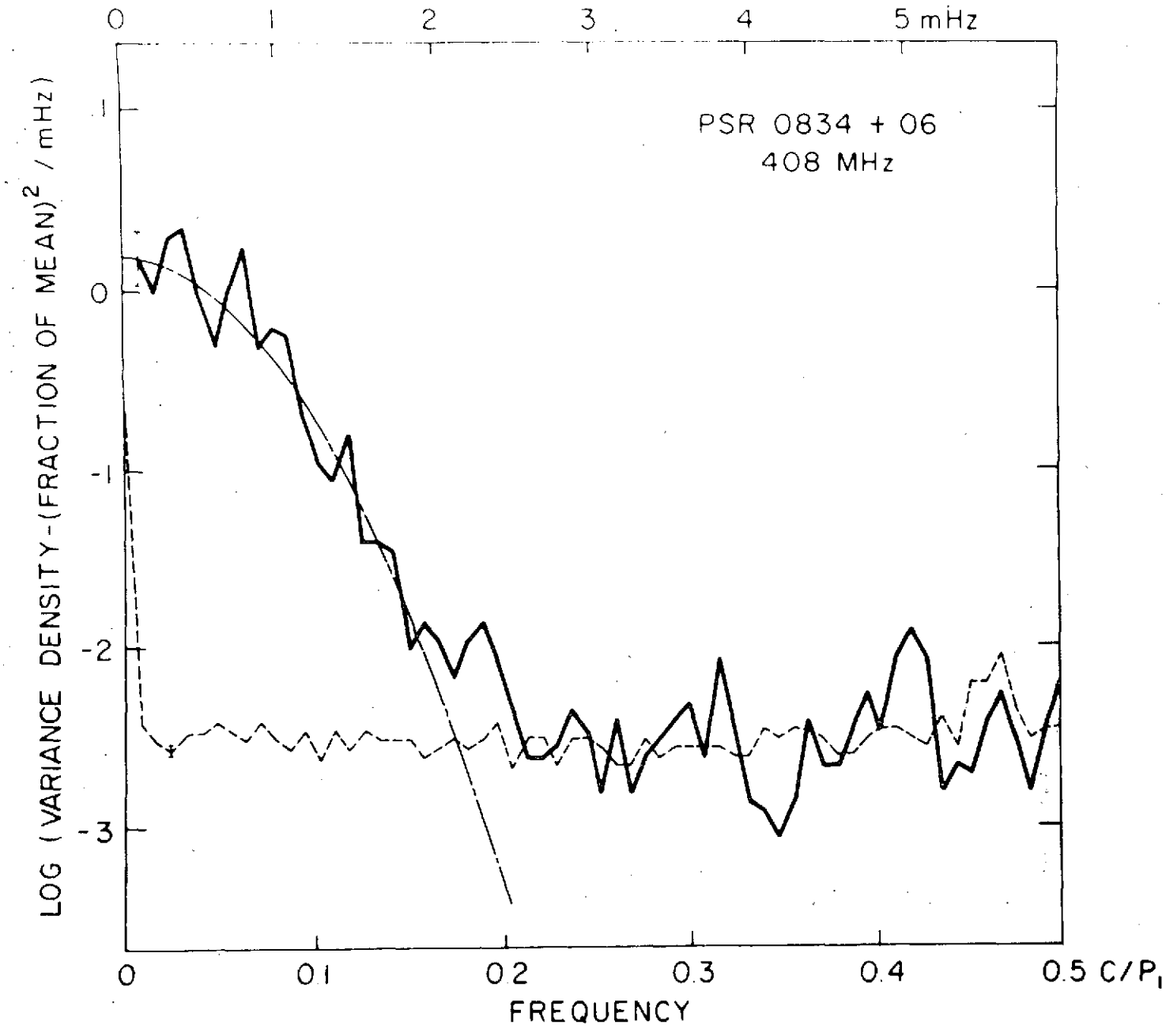
0
1
2
3
4
5 mHz
PSR 0834 + 06
408 MHz
LOG (VARIANCE DENSITY-(FRACTION OF MEAN)^2 / mHz)
1
0
-1
-2
-3
0
0.1
0.2
0.3
0.4
0.5 C/P$_1$
FREQUENCY

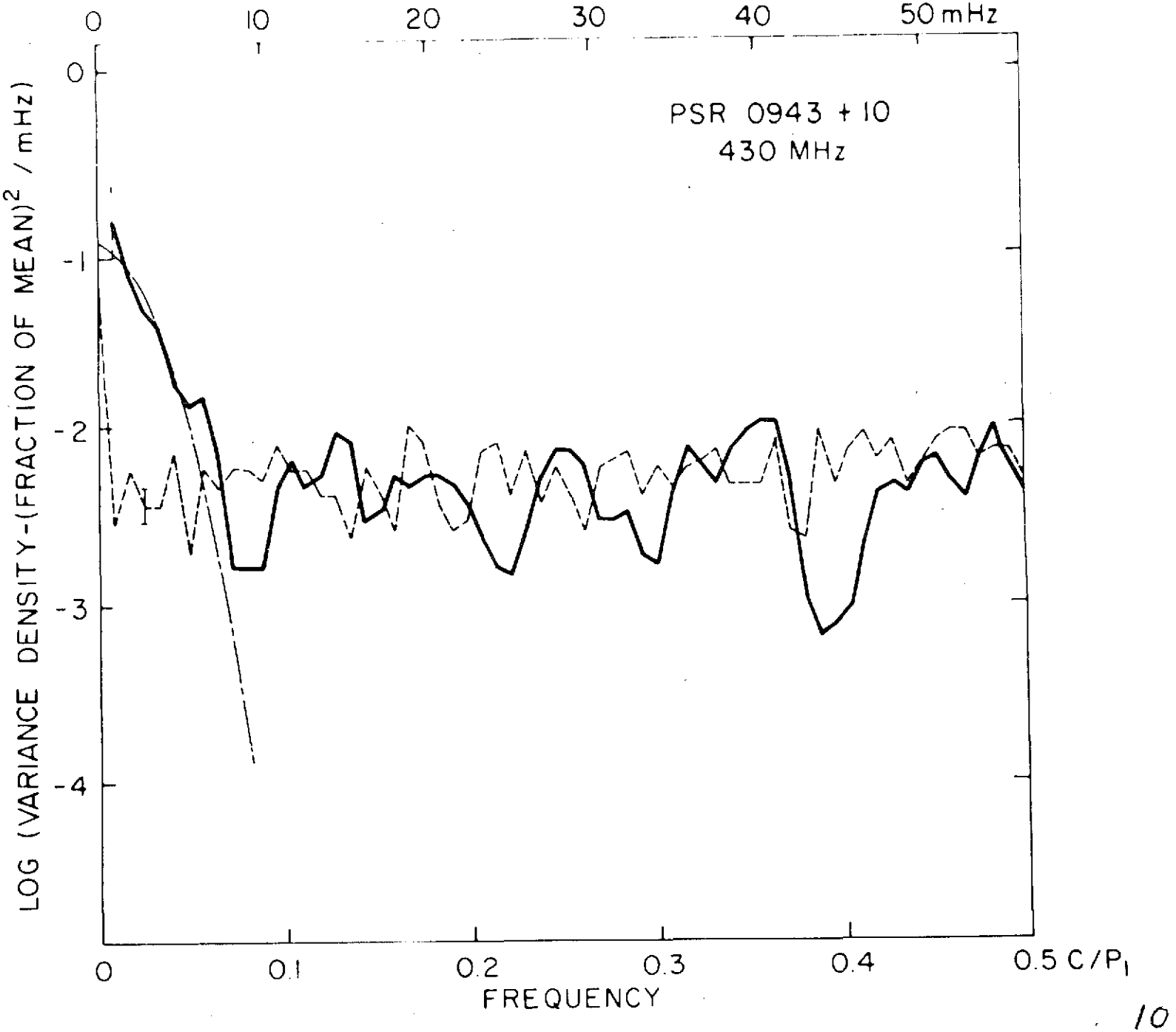
0
10
20
30
40
50 mHz
PSR 0943 + 10
430 MHz
LOG (VARIANCE DENSITY-(FRACTION OF MEAN)^2 / mHz)
-1
-2
-3
-4
0
0.1
0.2
0.3
0.4
0.5 C/P$_1$
FREQUENCY

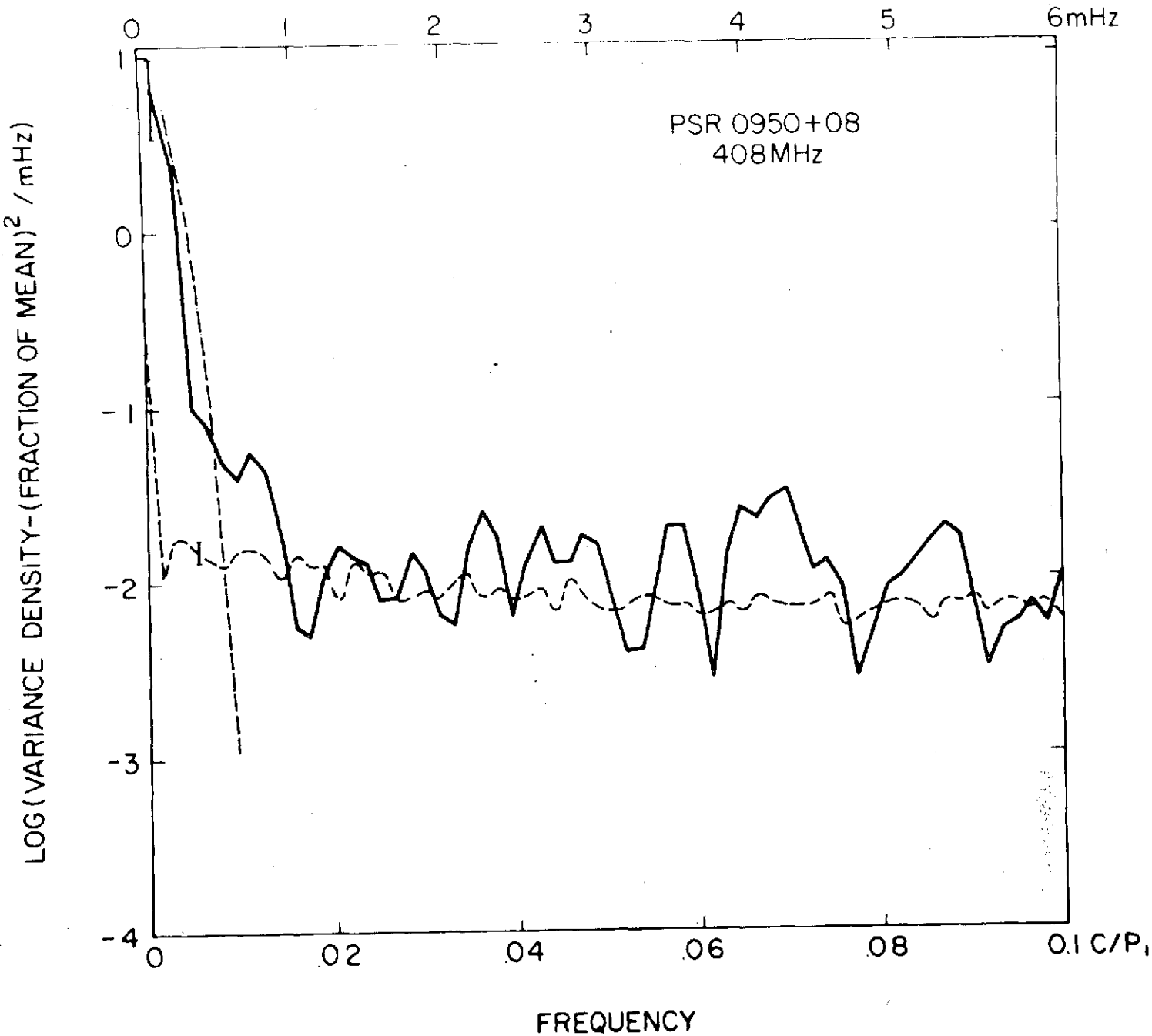
0
1
2
3
4
5
6mHz
PSR 0950+08
408MHz
LOG(VARIANCE DENSITY-(FRACTION OF MEAN)^2 / mHz)
1
0
-1
-2
-3
-4
0
.02
.04
.06
.08
0.1 C/P$_1$
FREQUENCY

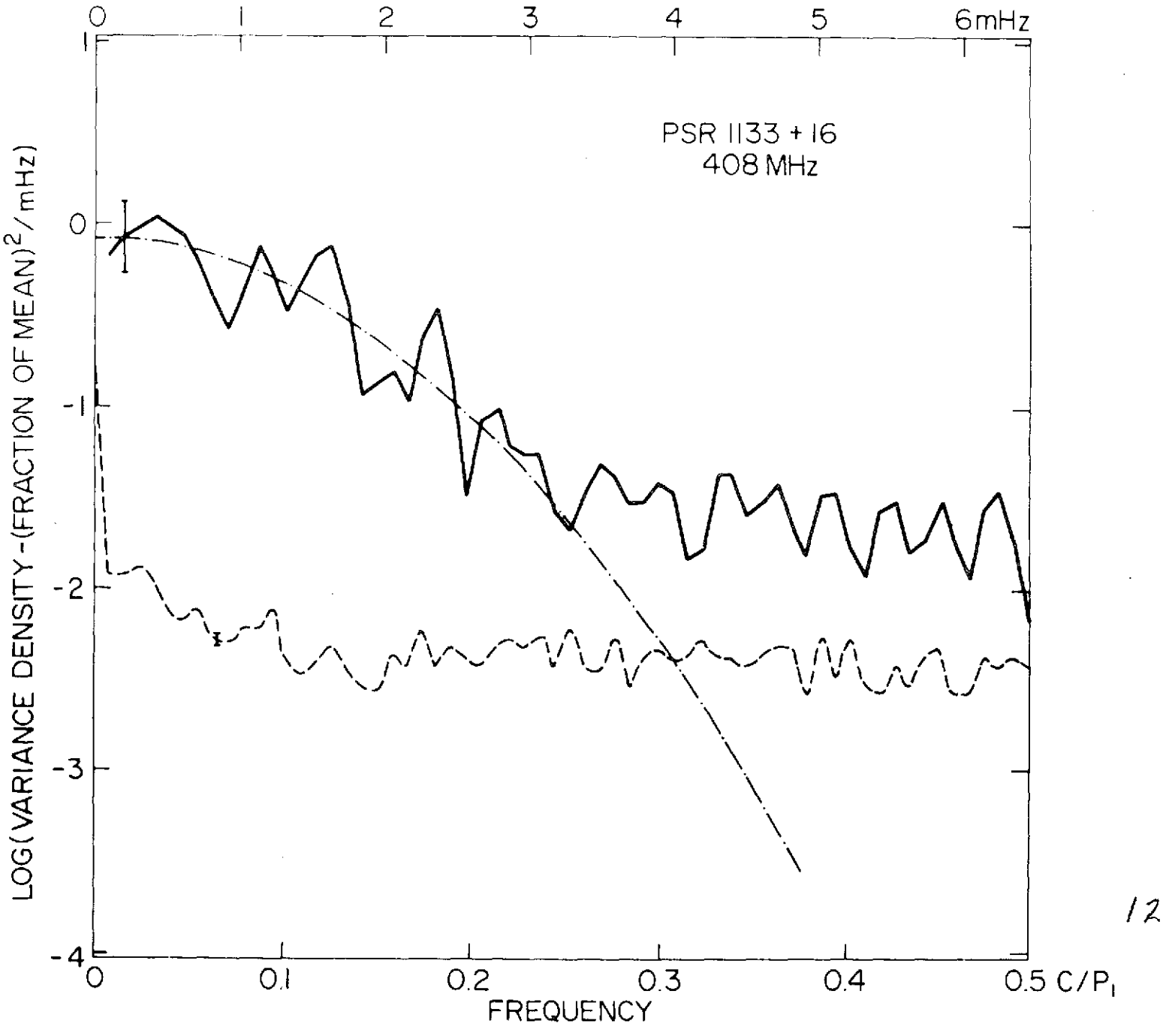
0
1
2
3
4
5
6mHz
PSR 1133 + 16
408 MHz
LOG(VARIANCE DENSITY - (FRACTION OF MEAN)^2/mHz)
1
0
-1
-2
-3
-4
0
0.1
0.2
0.3
0.4
0.5 C/P$_1$
FREQUENCY

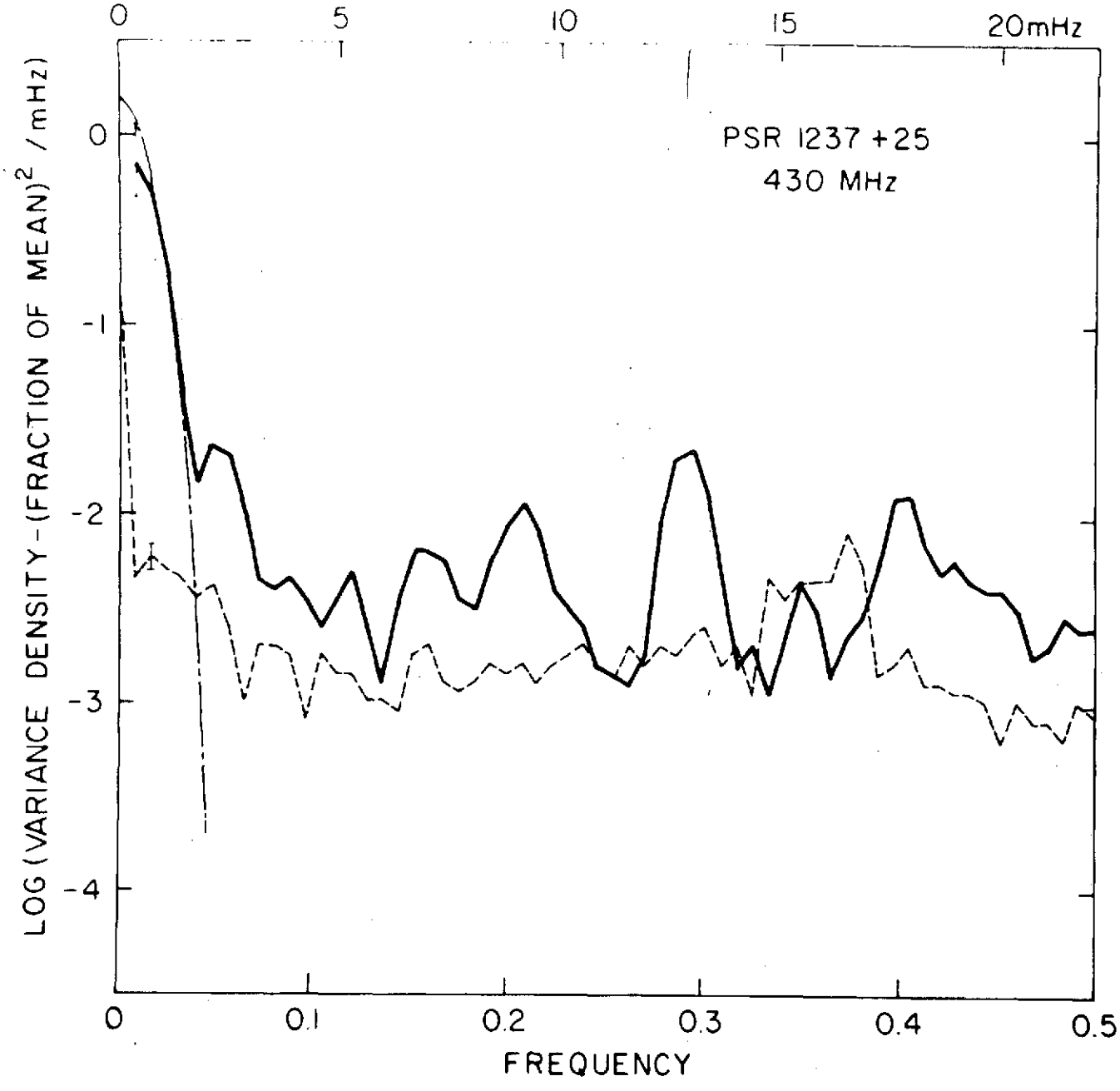
0
5
10
15
20mHz
PSR 1237 +25
430 MHz
LOG (VARIANCE DENSITY-(FRACTION OF MEAN)^2 / mHz)
0
-1
-2
-3
-4
0
0.1
0.2
0.3
0.4
0.5
FREQUENCY

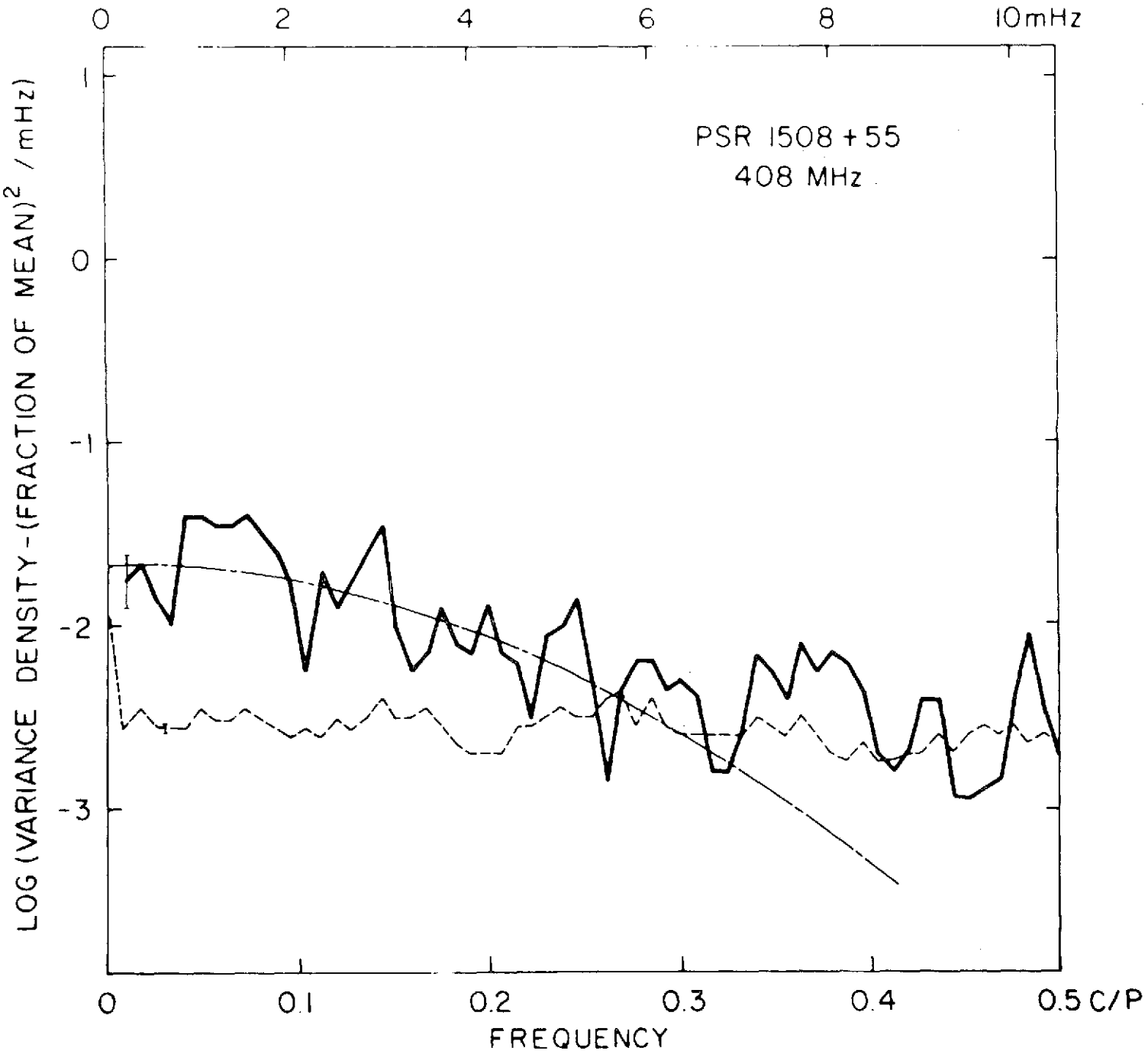
0
2
4
6
8
10mHz
1
0
-1
-2
-3
PSR 1508+55
408 MHz
LOG (VARIANCE DENSITY-(FRACTION OF MEAN)^2 / mHz)
0
0.1
0.2
0.3
0.4
0.5 C/P$_1$
FREQUENCY

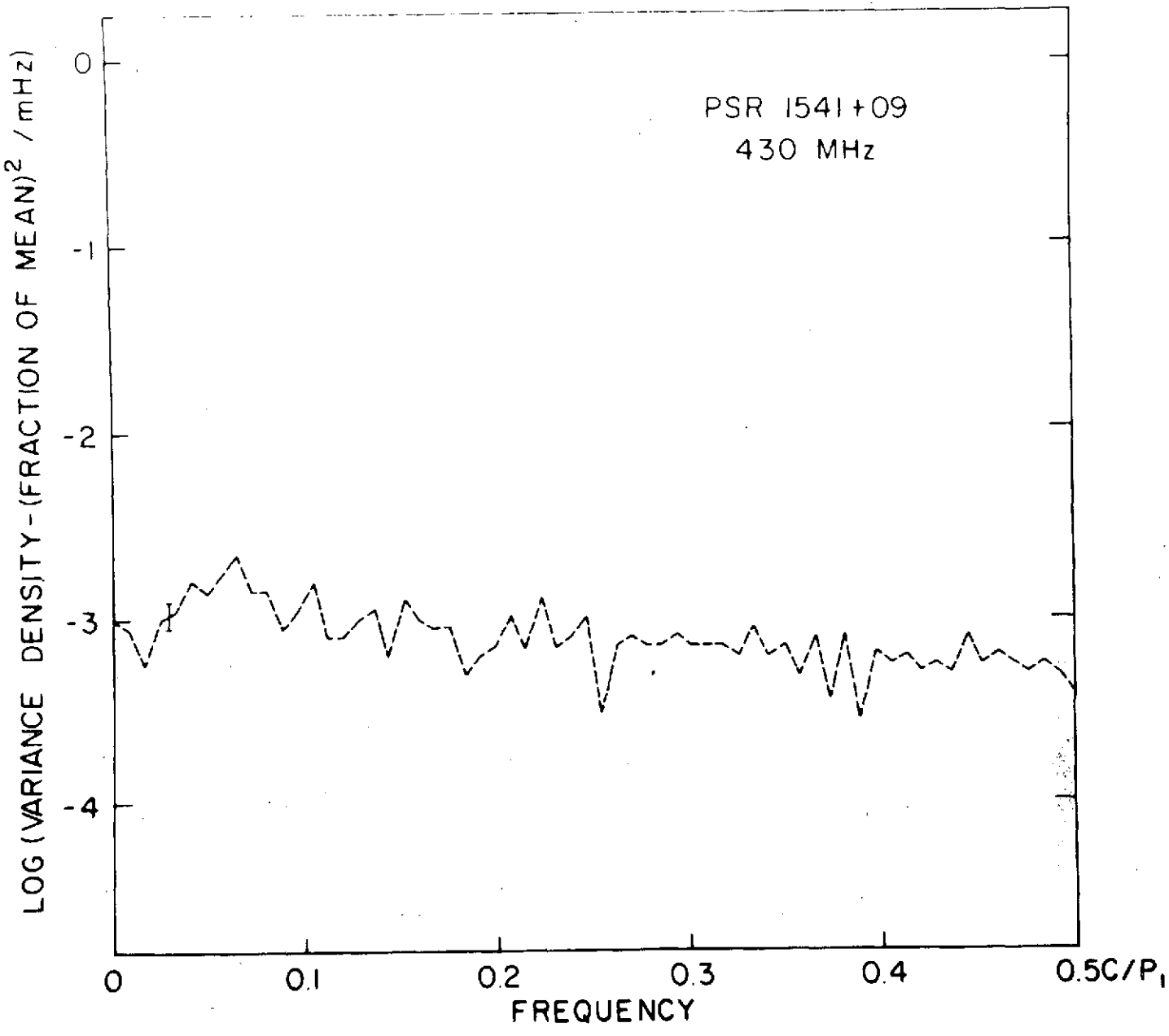
PSR 1541+09
430 MHz
LOG (VARIANCE DENSITY - (FRACTION OF MEAN)^2 / mHz)
0
-1
-2
-3
-4
0
0.1
0.2
0.3
0.4
0.5C/P$_1$
FREQUENCY

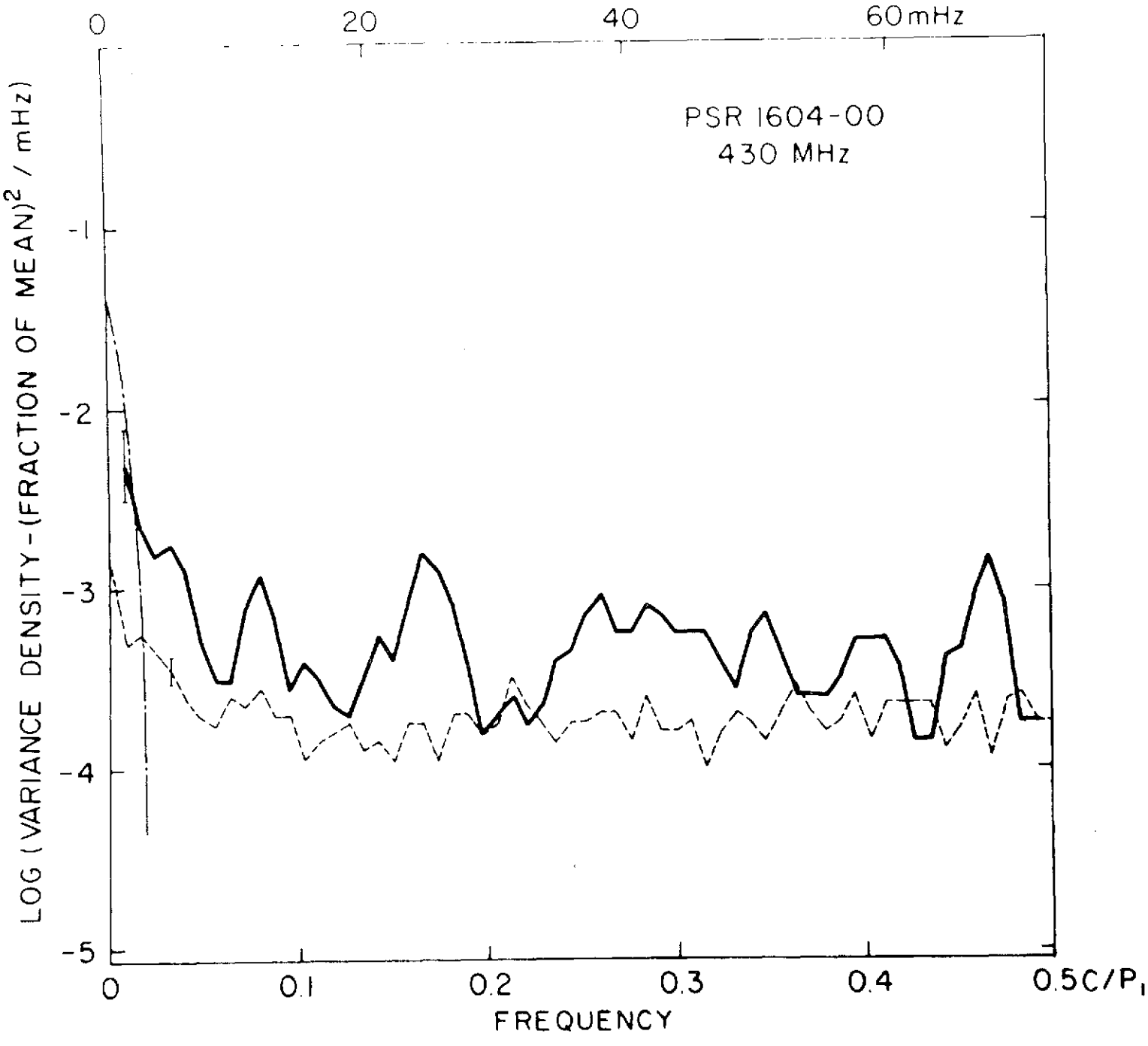
0
20
40
60 mHz
PSR 1604-00
430 MHz
LOG (VARIANCE DENSITY - (FRACTION OF MEAN)^2 / mHz)
-1
-2
-3
-4
-5
0
0.1
0.2
0.3
0.4
0.5 C/P$_1$
FREQUENCY

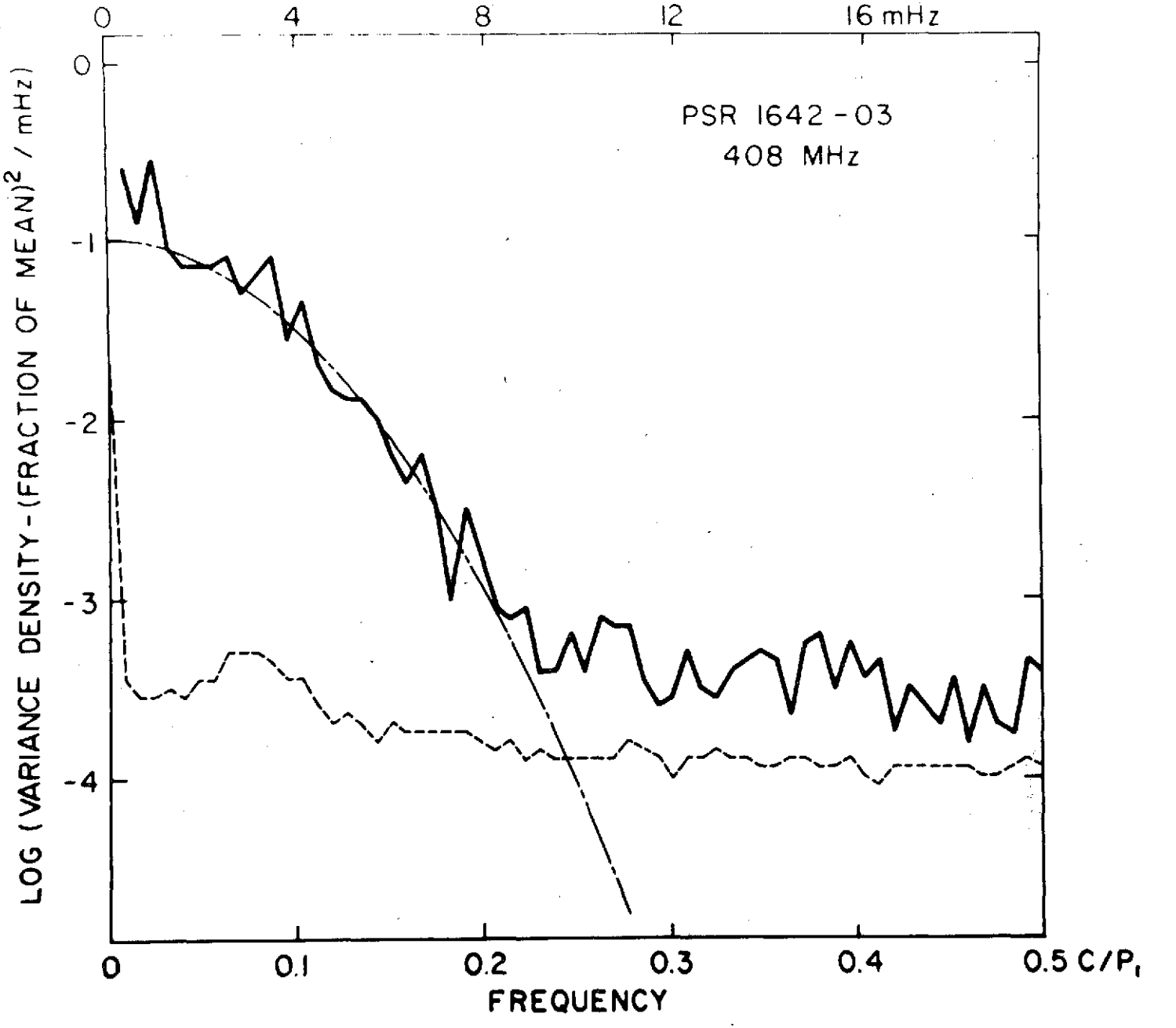
0
4
8
12
16 mHz
PSR 1642 - 03
408 MHz
LOG (VARIANCE DENSITY - (FRACTION OF MEAN)² / mHz)
0
-1
-2
-3
-4
0
0.1
0.2
0.3
0.4
0.5 C/P₁
FREQUENCY

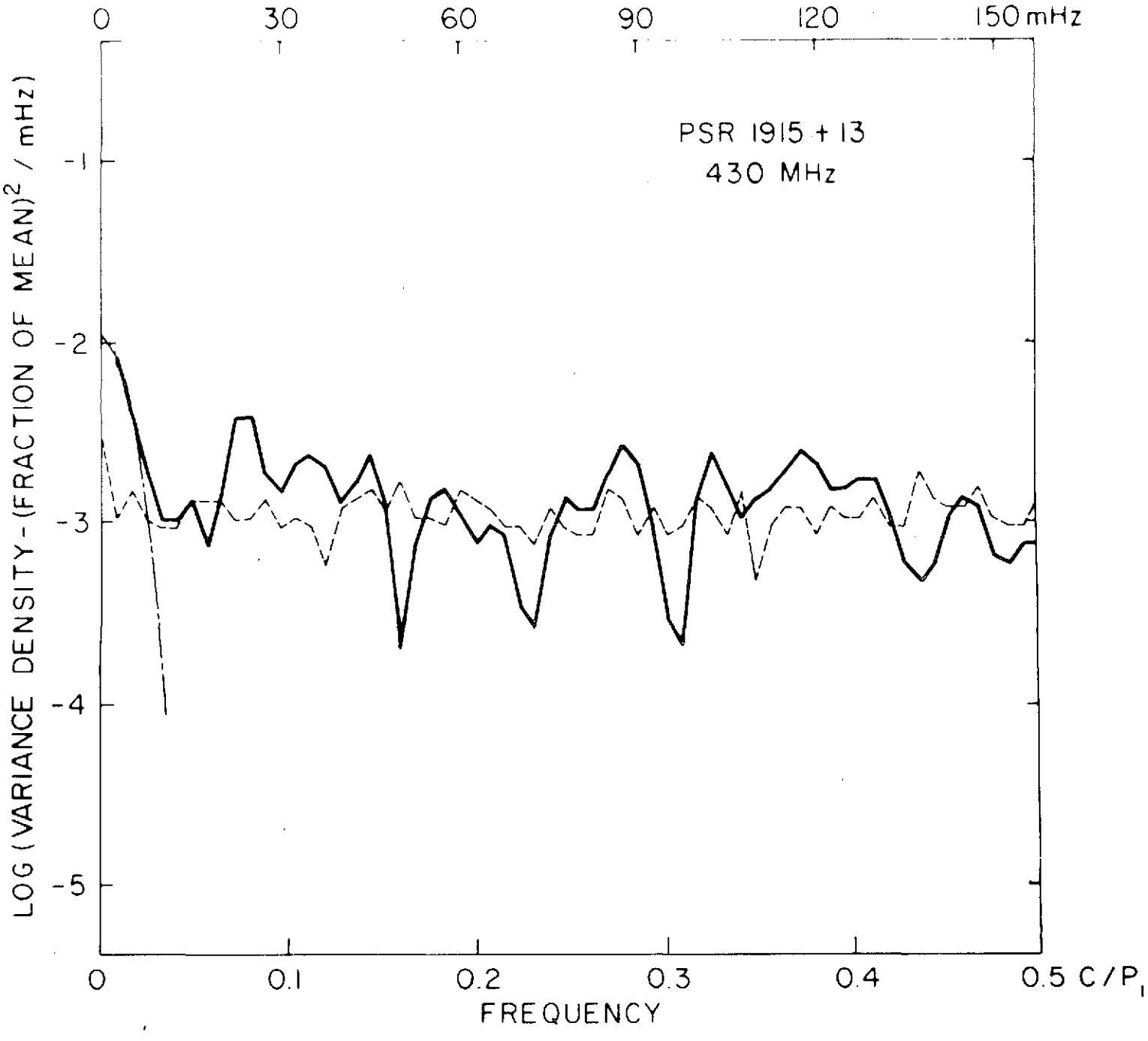
0
30
60
90
120
150 mHz
PSR 1915 + 13
430 MHz
LOG (VARIANCE DENSITY - (FRACTION OF MEAN)^2 / mHz)
-1
-2
-3
-4
-5
0
0.1
0.2
0.3
0.4
0.5 C/P$_1$
FREQUENCY

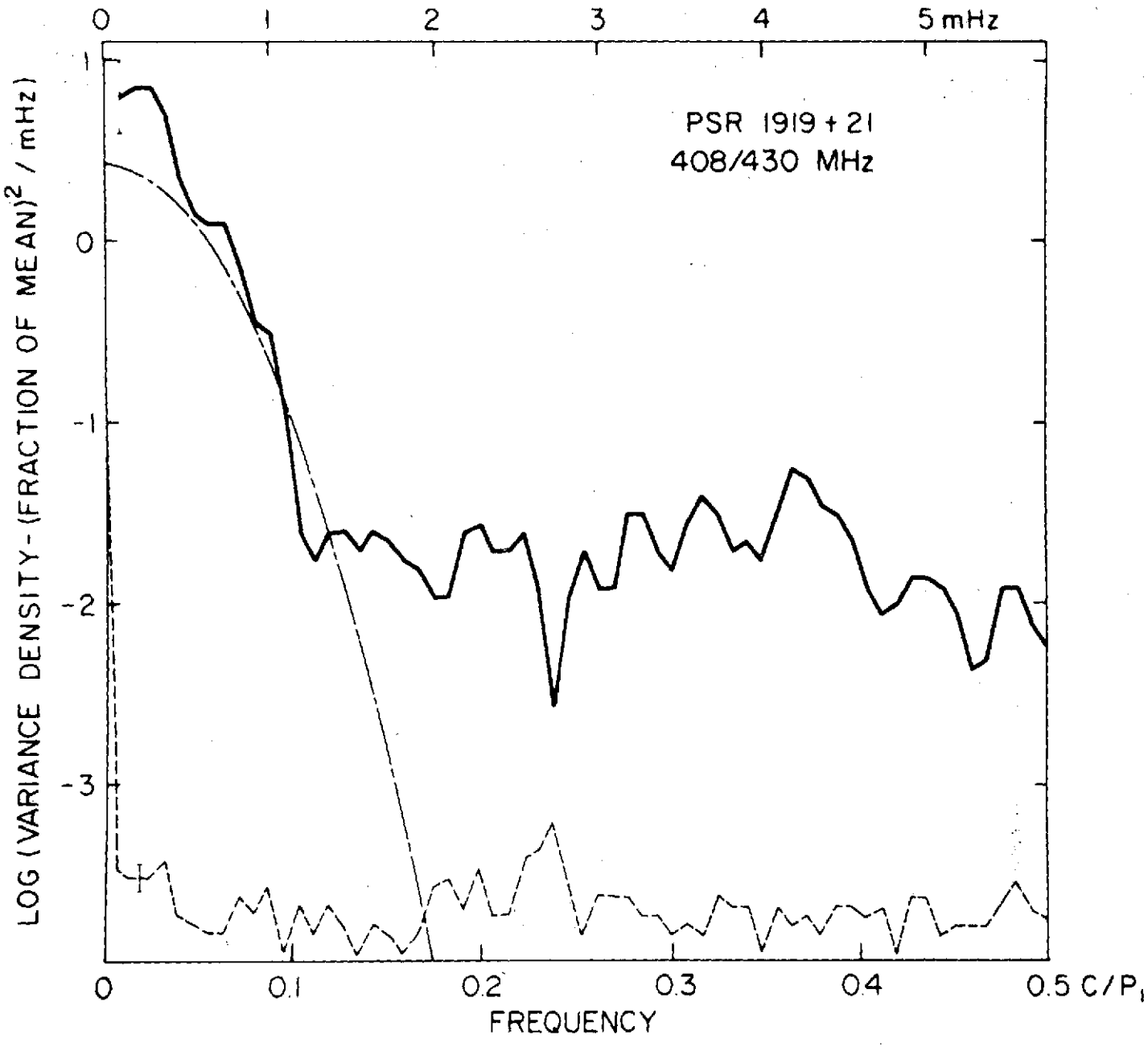
0
1
2
3
4
5 mHz
PSR 1919 + 21
408/430 MHz
LOG (VARIANCE DENSITY - (FRACTION OF MEAN)² / mHz)
1
0
-1
-2
-3
0
0.1
0.2
0.3
0.4
0.5 C/P₁
FREQUENCY

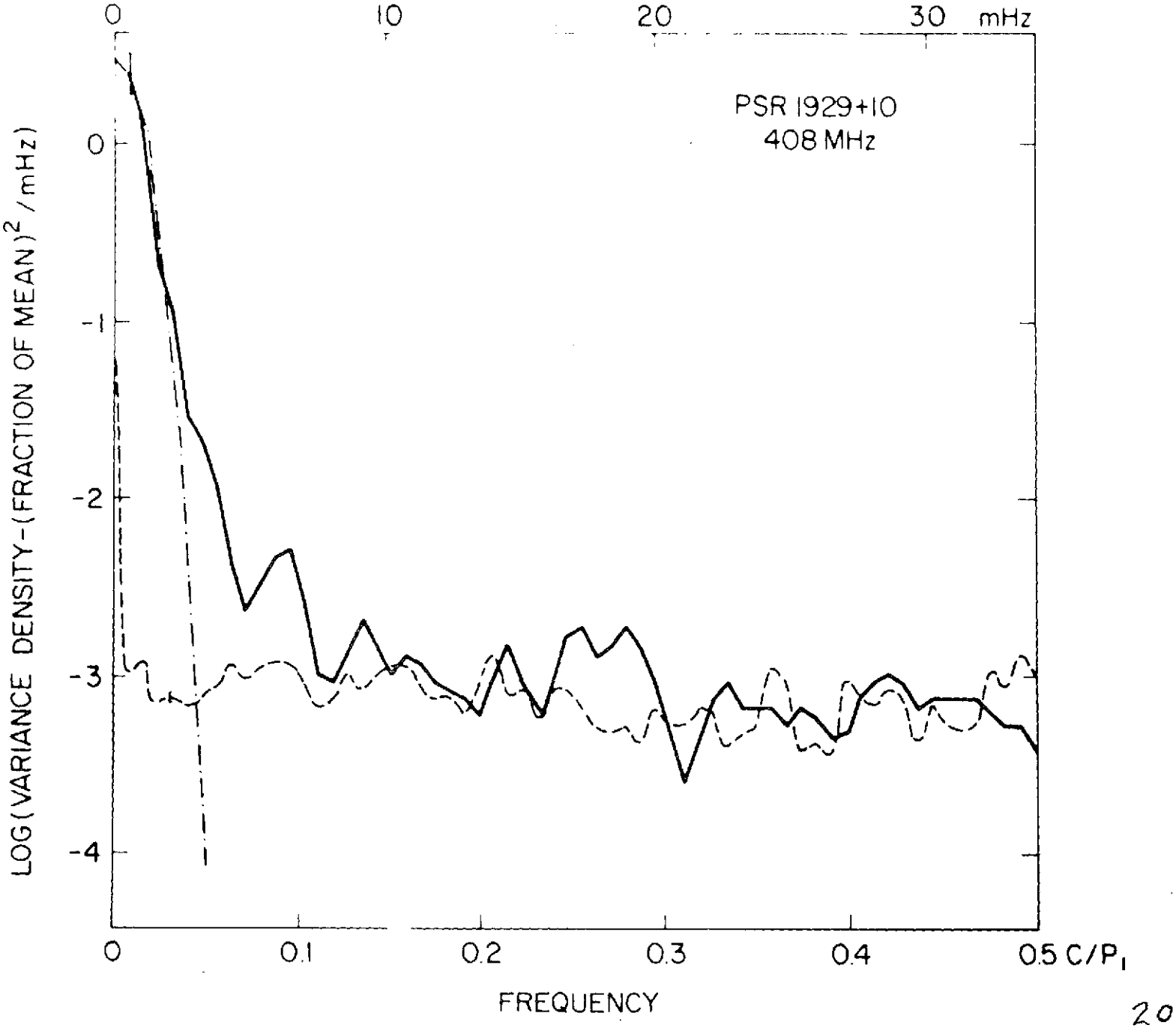
0
10
20
30 mHz
PSR 1929+10
408 MHz
0
-1
-2
-3
-4
LOG (VARIANCE DENSITY - (FRACTION OF MEAN)^2 / mHz)
0
0.1
0.2
0.3
0.4
0.5 C/P$_1$
FREQUENCY

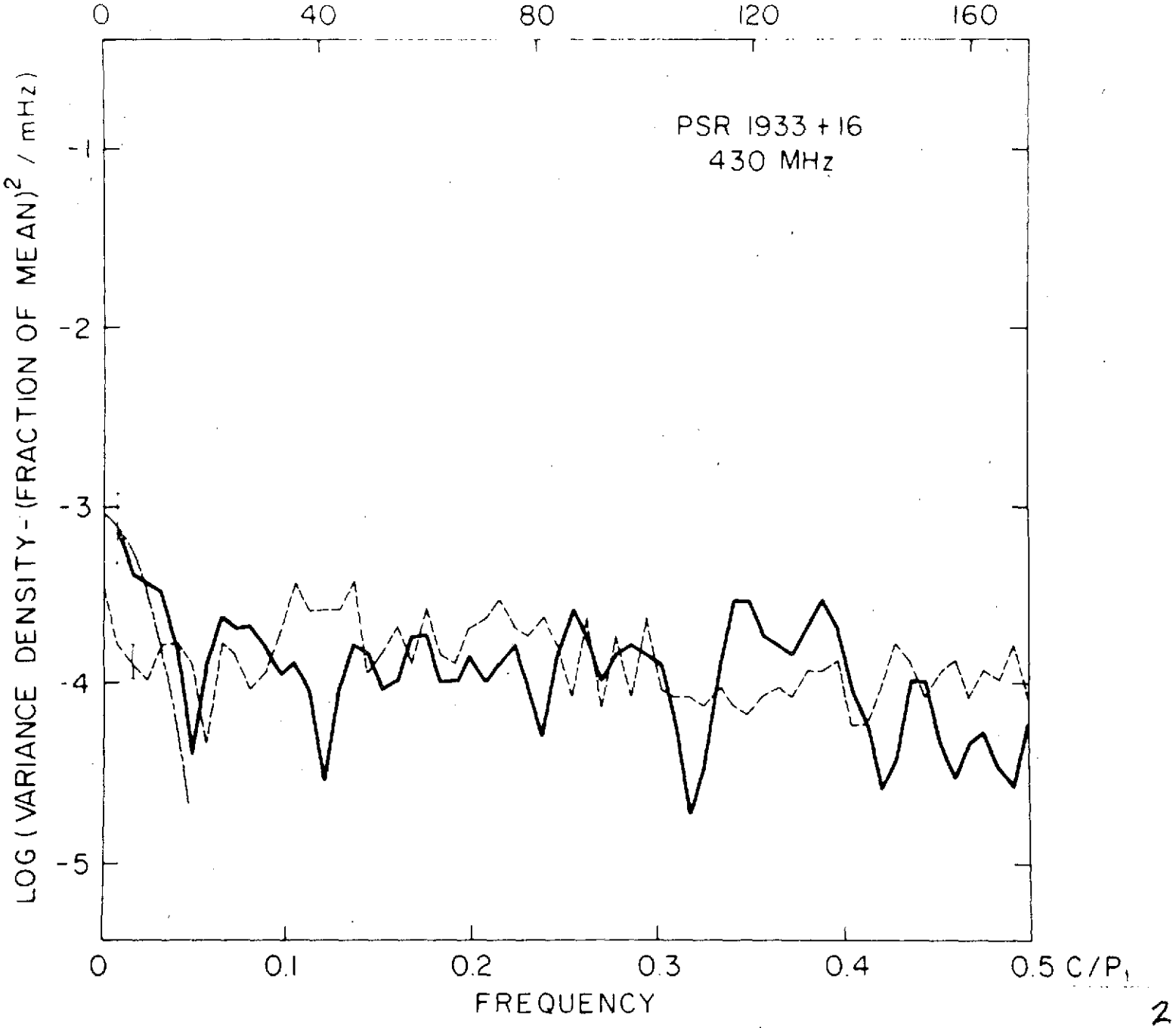
0
40
80
120
160
PSR 1933 + 16
430 MHz
LOG (VARIANCE DENSITY - (FRACTION OF MEAN)^2 / mHz)
-1
-2
-3
-4
-5
0
0.1
0.2
0.3
0.4
0.5 C/P$_1$
FREQUENCY

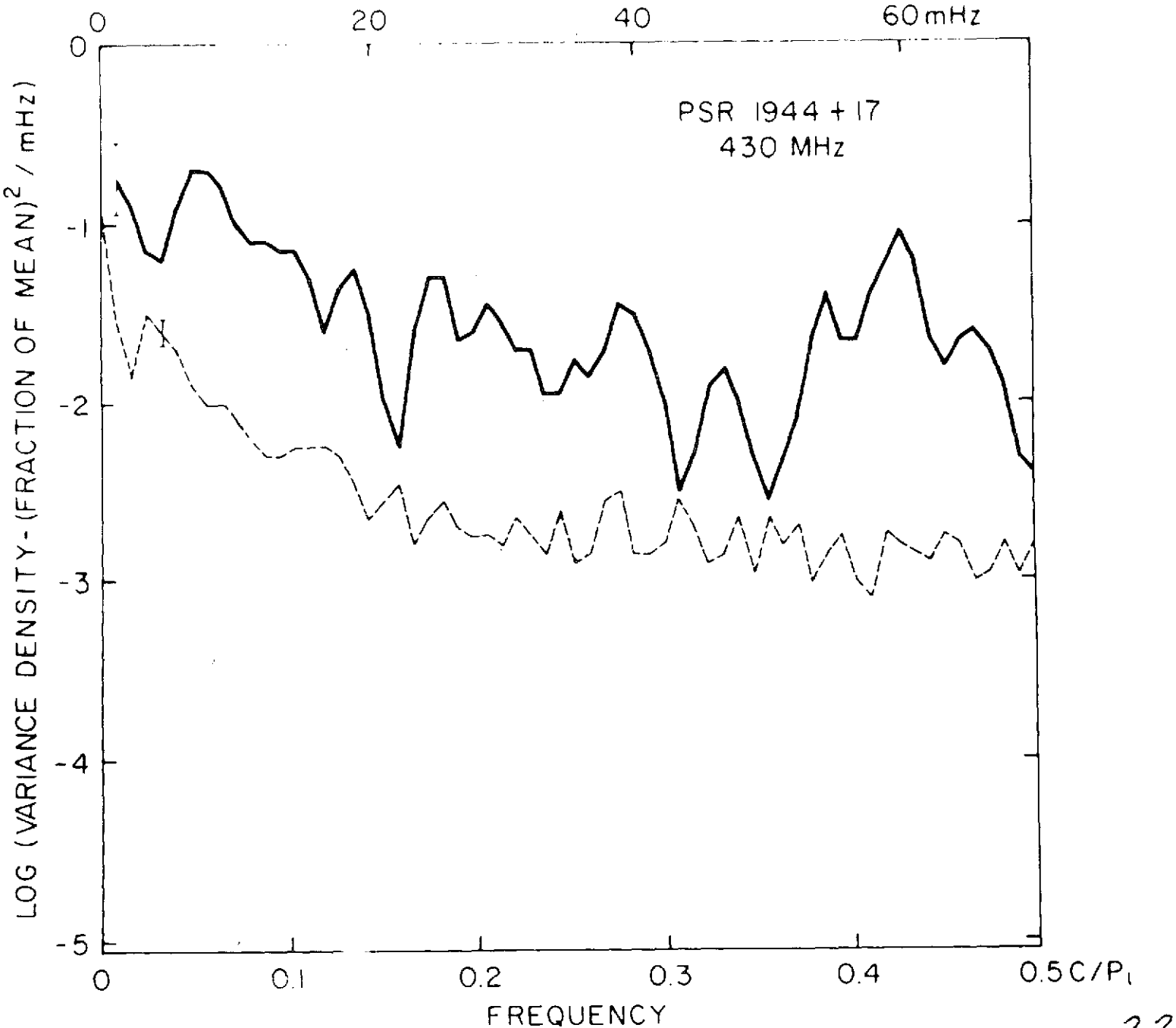
0
20
40
60 mHz
PSR 1944 + 17
430 MHz
LOG (VARIANCE DENSITY - (FRACTION OF MEAN)^2 / mHz)
-1
-2
-3
-4
-5
0
0.1
0.2
0.3
0.4
0.5 C/P$_1$
FREQUENCY

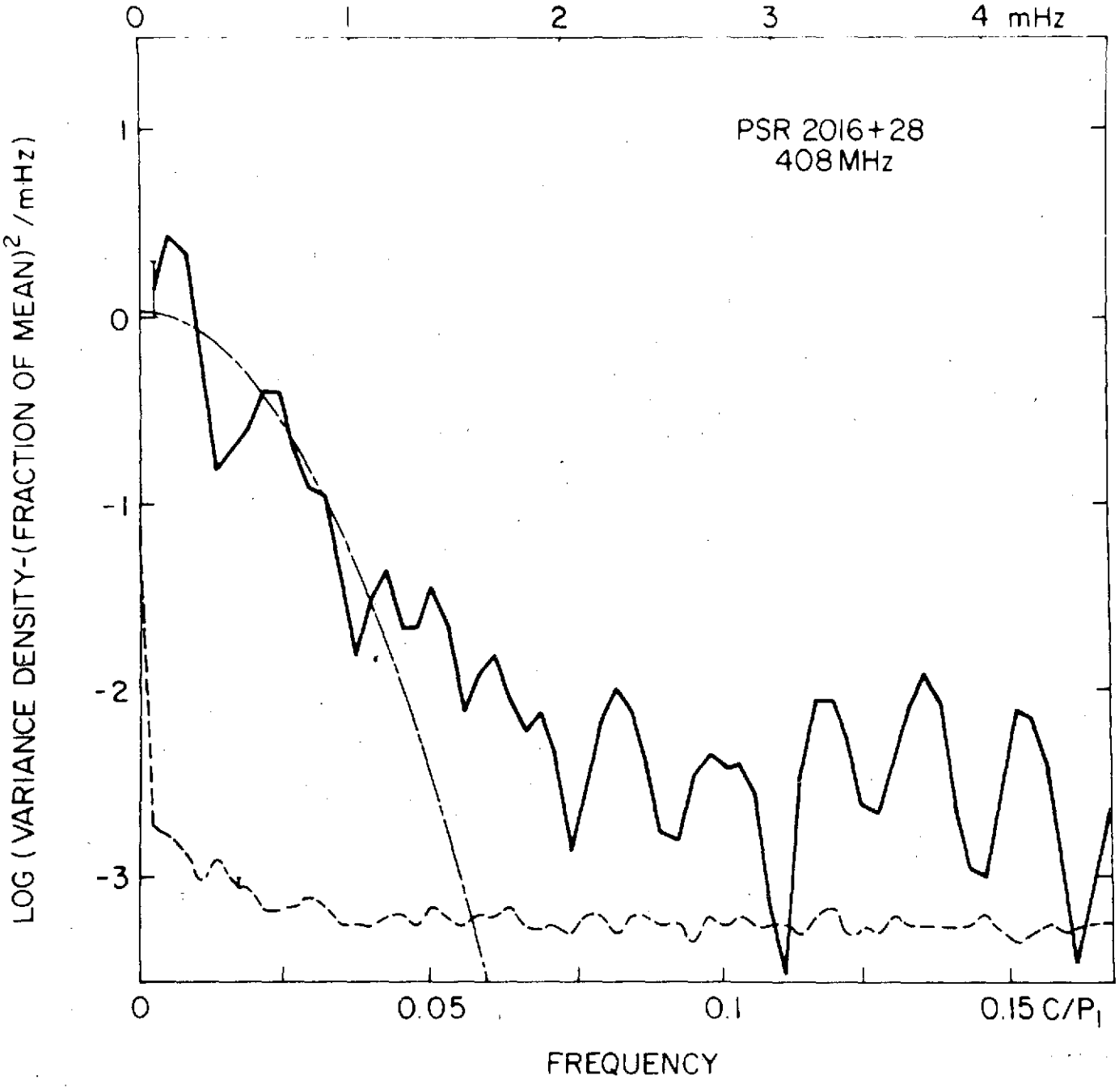
0
1
2
3
4 mHz
PSR 2016+28
408 MHz
LOG (VARIANCE DENSITY-(FRACTION OF MEAN)^2 /mHz)
1
0
-1
-2
-3
0
0.05
0.1
0.15 C/P$_1$
FREQUENCY

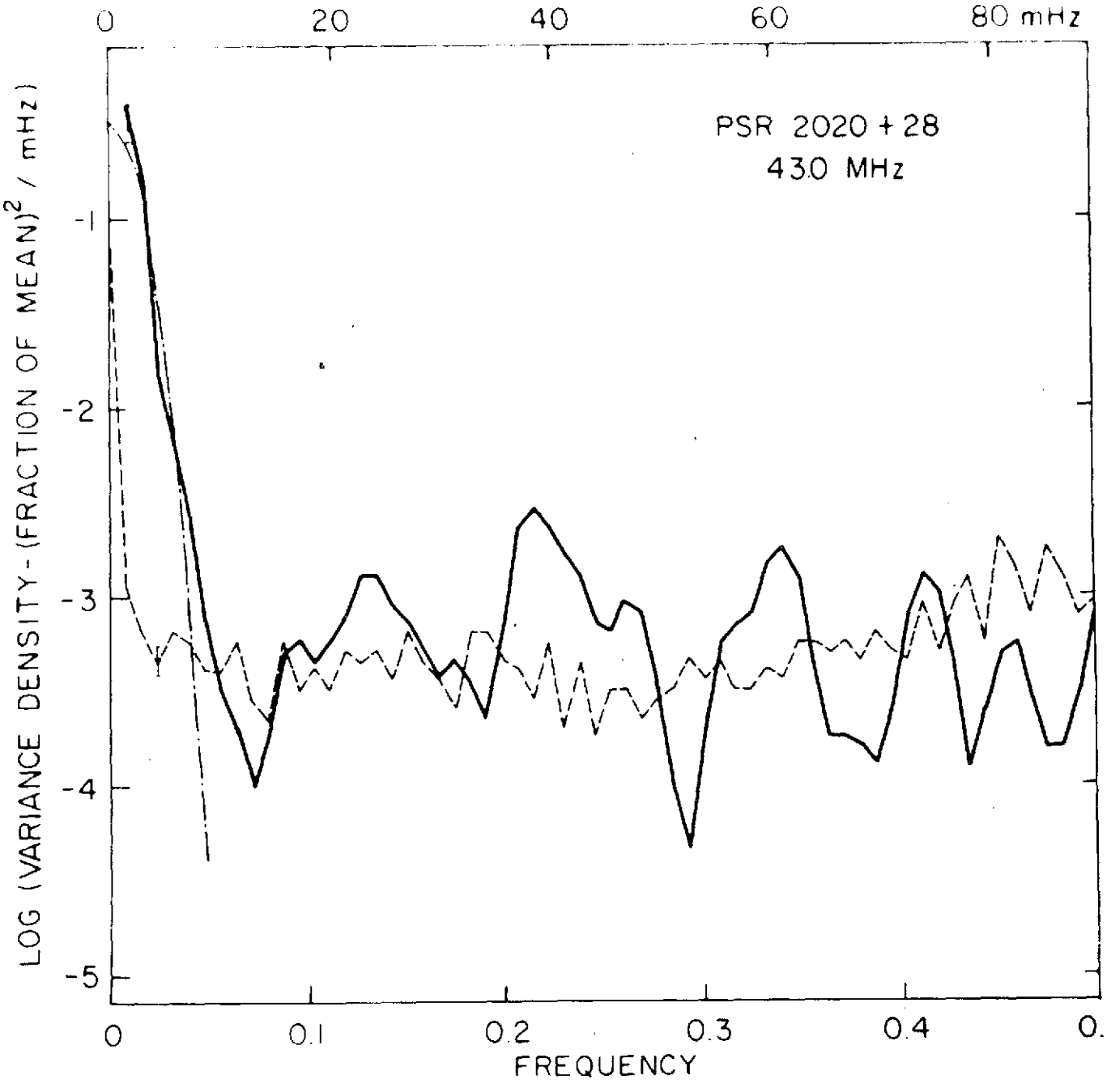
0
20
40
60
80 mHz
PSR 2020 + 28
430 MHz
LOG (VARIANCE DENSITY - (FRACTION OF MEAN)^2 / mHz)
-1
-2
-3
-4
-5
0
0.1
0.2
0.3
0.4
0.5 C/P$_1$
FREQUENCY

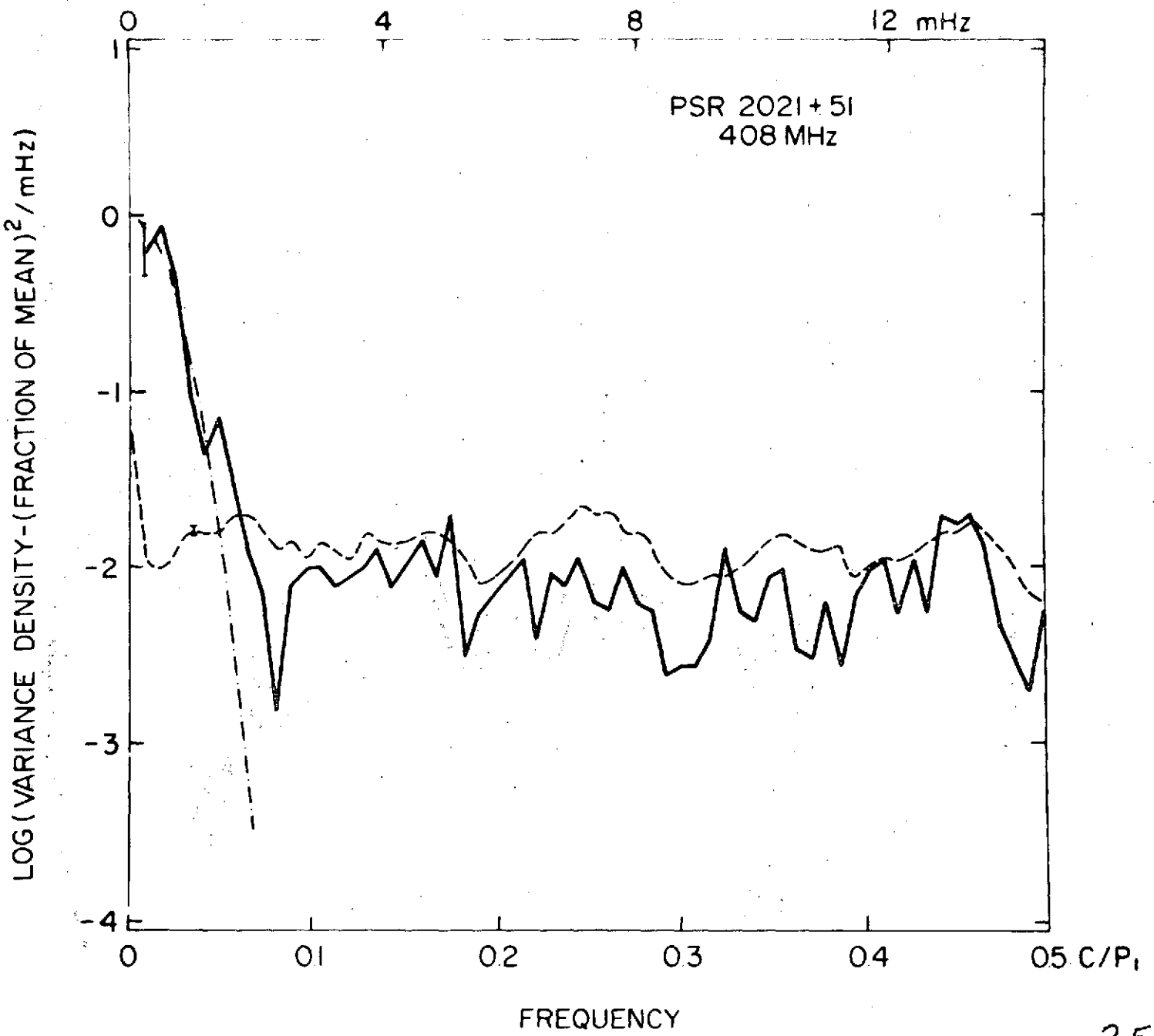
0
4
8
12 mHz
PSR 2021+51
408 MHz
LOG (VARIANCE DENSITY-(FRACTION OF MEAN)²/mHz)
1
0
-1
-2
-3
-4
0
01
02
03
04
05 C/P₁
FREQUENCY

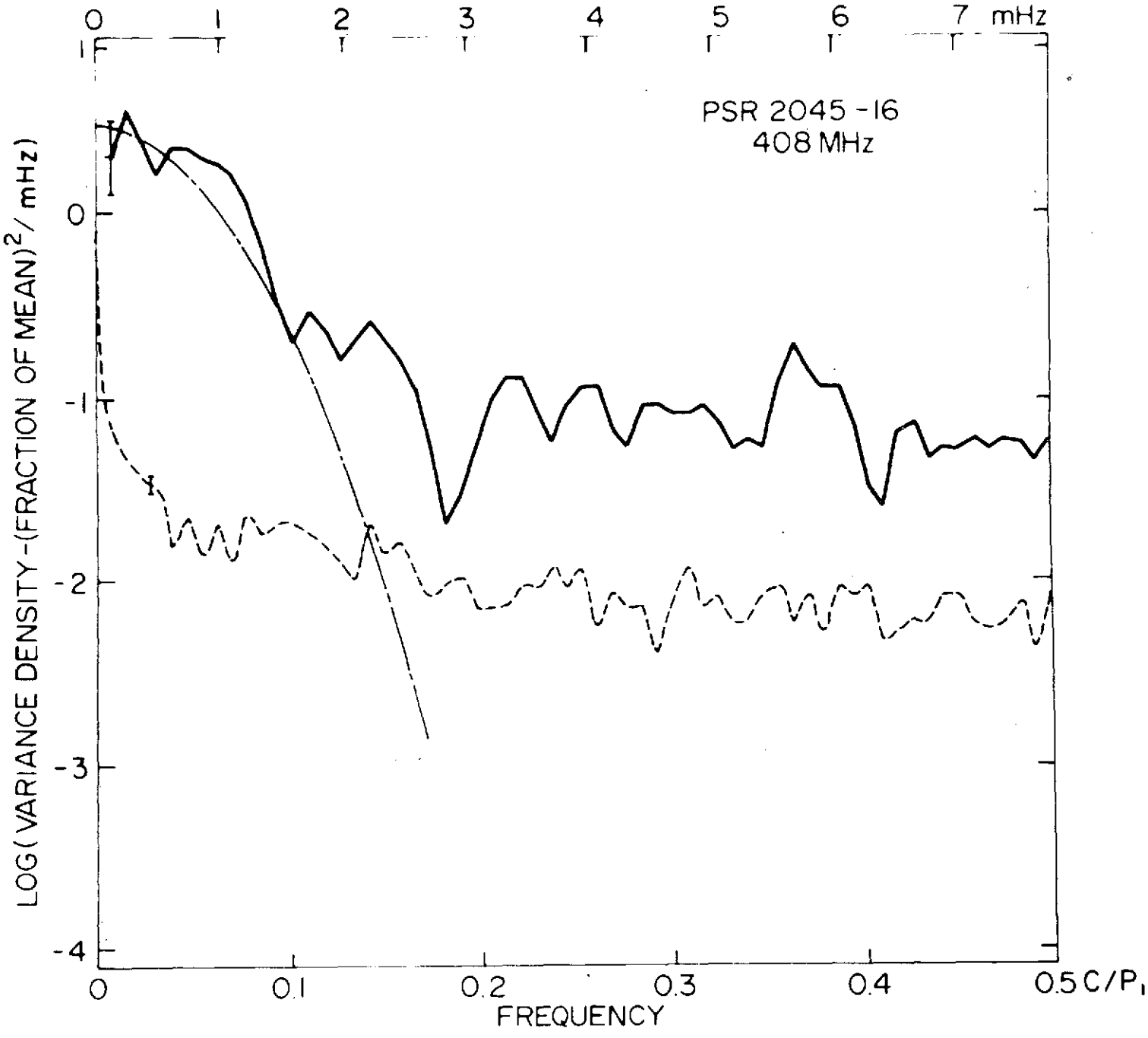
0 1 2 3 4 5 6 7 mHz
F
PSR 2045 -16
408 MHz
LOG (VARIANCE DENSITY - (FRACTION OF MEAN)² / mHz)
0
-1
-2
-3
-4
0
0.1
0.2
0.3
0.4
0.5 C/P₁
FREQUENCY

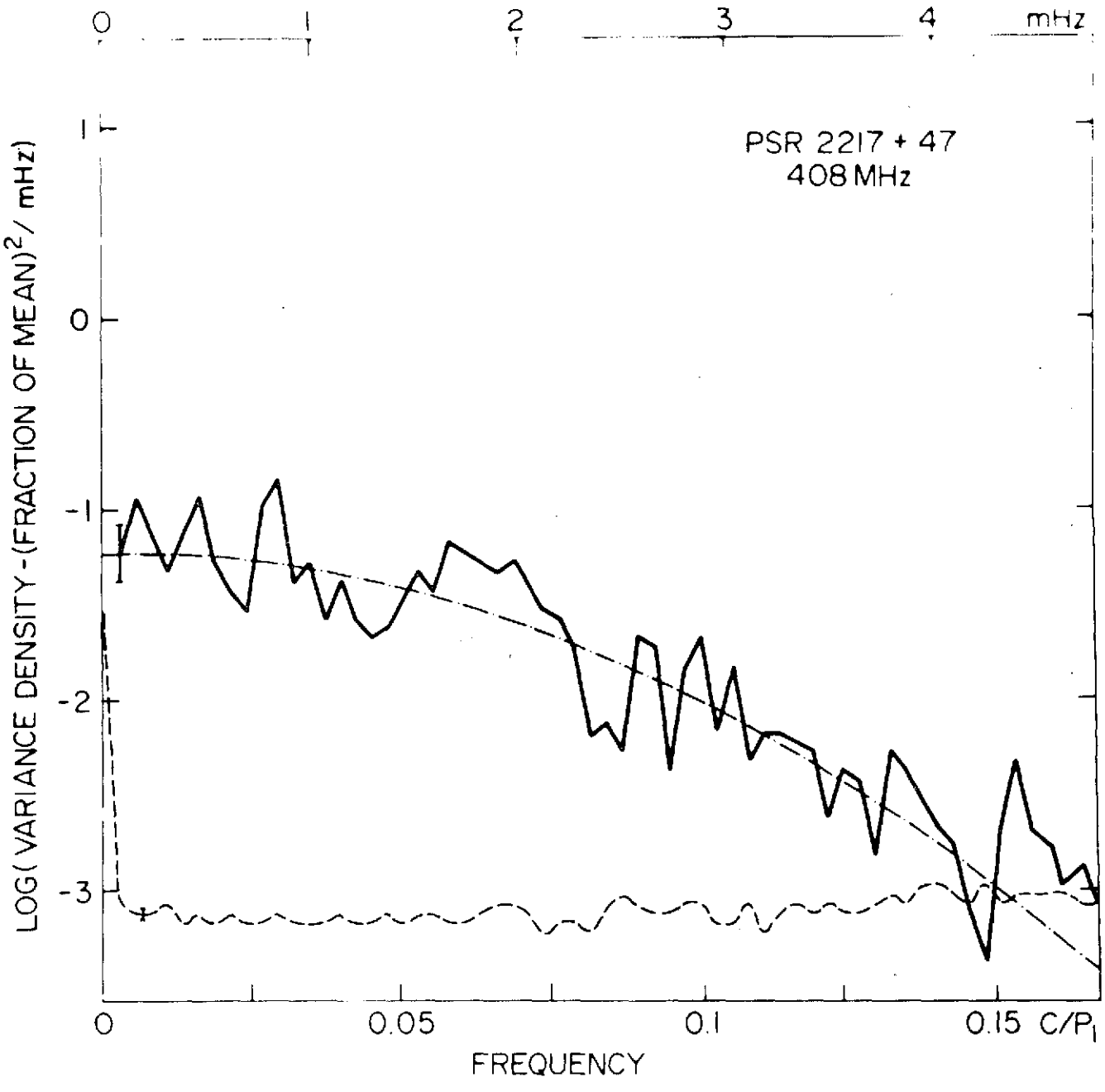
0
1
2
3
4
mHz
PSR 2217 + 47
408 MHz
LOG(VARIANCE DENSITY - (FRACTION OF MEAN)^2 / mHz)
1
0
-1
-2
-3
0
0.05
0.1
0.15 C/P$_1$
FREQUENCY

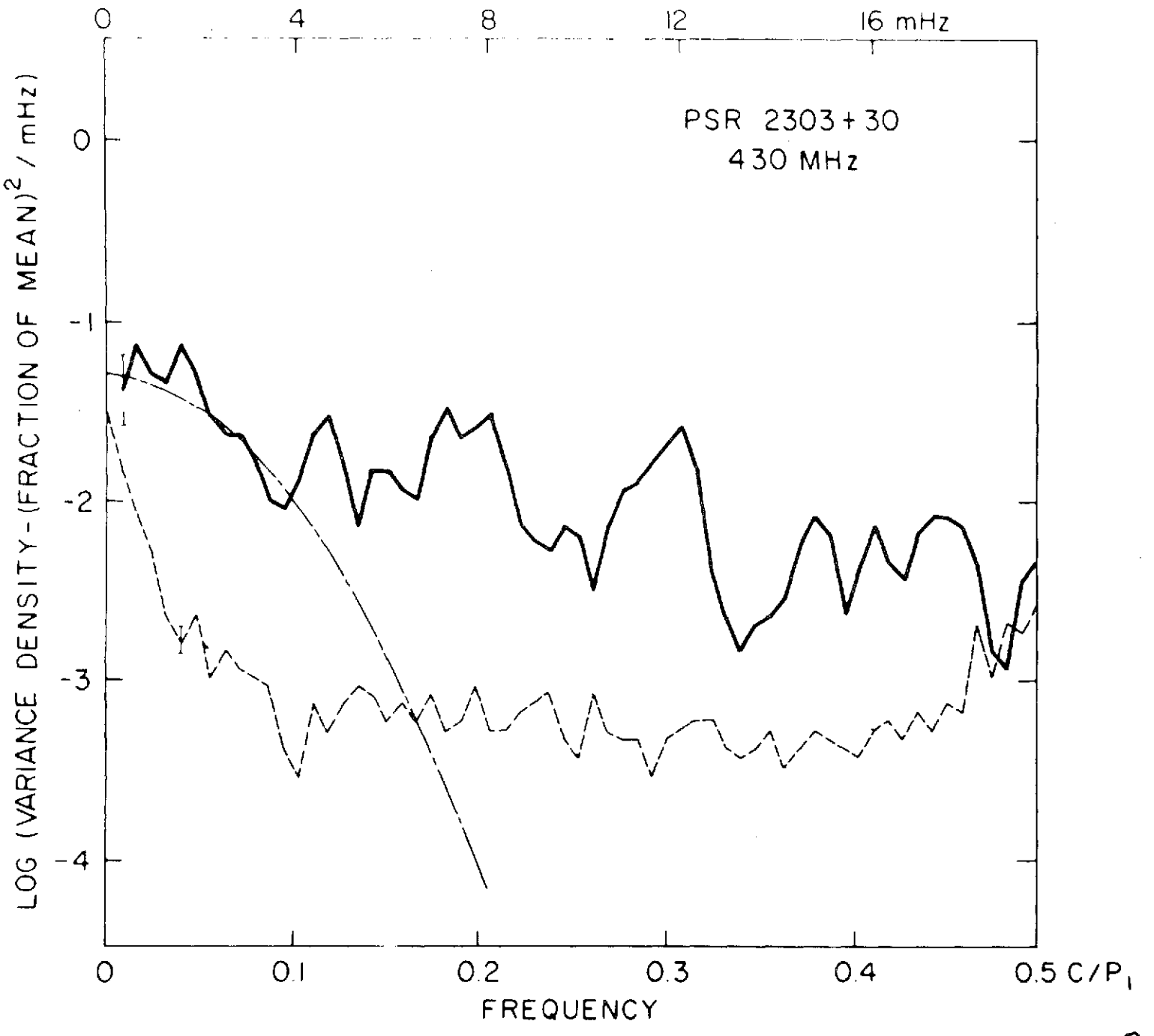
0
4
8
12
16 mHz
PSR 2303+30
430 MHz
LOG (VARIANCE DENSITY-(FRACTION OF MEAN)^2 / mHz)
0
-1
-2
-3
-4
0
0.1
0.2
0.3
0.4
0.5 C/P$_1$
FREQUENCY